Journal for
Occultation Astronomy

Volume 12 · No. 2 2022-02

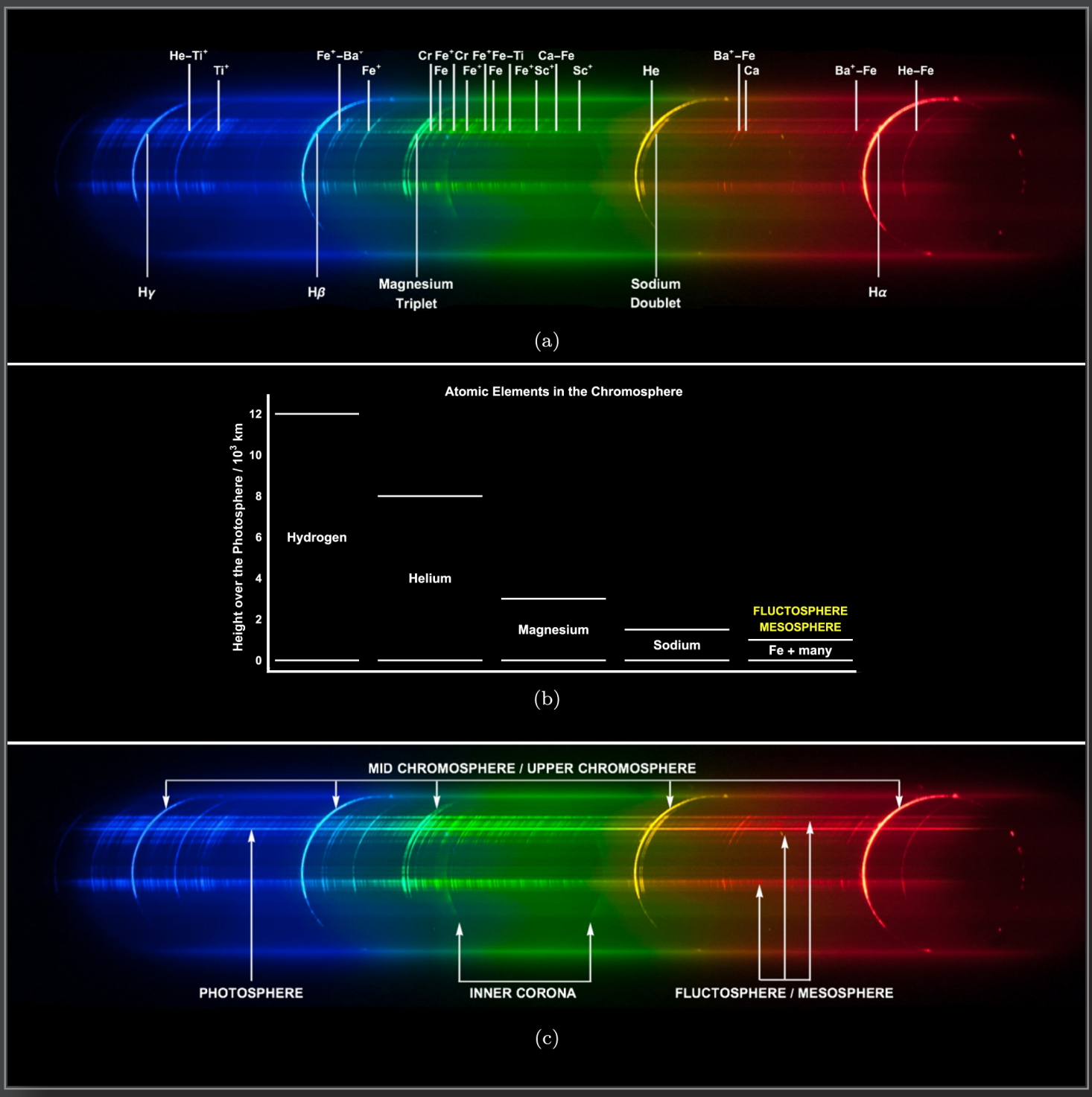

Measuring the Solar Radius with Flash Spectrum Videos

Dear reader,

Now exactly 40 years ago, I got my first two positive asteroidal occultations, visually observed, of course. With an analogue stopwatch in hand and acoustic time beeps as a background sound, who could have imagined the great knowledge we would accumulate with the occultations. Thanks to occultations we not only determine with high precision the position, size and shape of the objects, but they have also allowed us to discover satellites of these asteroids, rings, atmospheres, and as a derivative the albedo and density, which help us to determine their composition. Furthermore, occultations are almost the only viable source of characterisation for Trans-Neptunian Objects.

And let's not forget that in the case of the Sun, the same occultation timing technique applied to the Baily's Beads allows us to determine the solar radius. Or sometimes the surprise appears at the occulted star in the form of the discovery of unknown stellar components.

Forty years ago, even predictions of grazing occultations by the Moon were very inaccurate. I remember more than one expedition to the northern limit with a miss at all stations.

All the articles you can read in the present issue of JOA highlight these advances. They are efforts that do not go to the big headlines, but that help to do science in capital letters, and to discuss them with friends at every ESOP, like the next one in Granada.

Clear skies!

Carles Schnabel

IOTA/ES

JOA Volume 12 · No. 2 · 2022-2 $ 5.00 · $ 6.25 OTHER (ISSN 0737-6766)

In this Issue:

COVER

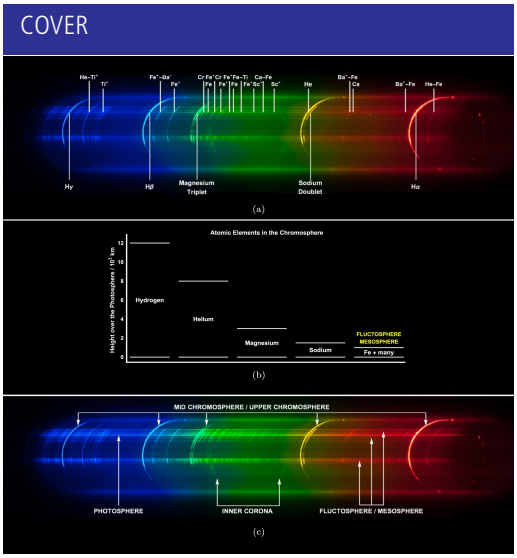

Detailed view of the flash spectrum. (a) The main emission lines are labelled with the elements that produce them. (b) Simplified view of the distribution of elements in the chromosphere (inspired by Mitchell, 1947). All elements are present, in measurable quantities, from the surface of the photosphere up to a certain height. (c) The photosphere generates an intense continuous spectrum (here just a thin line due to the last Baily's bead). The inner corona generates a ghostly diffuse spectrum. The mid and upper chromosphere only emits a few intense lines. The lower part of the chromosphere also emits a forest of faint lines besides the main intense ones, here predominately concentrated in the two lunar valleys of the last pair of Baily's beads. (K. Emmanouilidis, with permission by AAS)

Copyright Transfer

Rules for Authors

In order to optimise the publishing process, certain rules for authors have been set up how to write an article for *JOA*. They can be found in "How to Write an Article for *JOA*" published in this *JOA* issue (2018-3) on page 13. They also can be found on our webpage at http://www.iota-es.de/how2write_joa.html .

Journal for Occultation Astronomy

Estimating the Eclipse Solar Radius from Flash Spectrum Videos

Luca Quaglia · Sydney, New South Wales · Australia · besselianelements@gmail.com
John Irwin · Guildford, England · United Kingdom · john@jir1667.plus.com
Konstantinos Emmanouilidis · Thessaloniki · Greece · conemmil@gmail.com
Alessandro Pessi · Milan · Italy · issepela@gmail.com

ABSTRACT: The eclipse solar radius can be estimated by extracting Baily's beads light curves from flash spectrum videos recorded at the edge of the eclipse umbral shadow path and by fitting synthetic light curves onto them. The simulations are performed by integrating the limb darkening function over the exposed area of the photosphere. We have applied this methodology to the 2017 August 21 total solar eclipse and obtained an estimate $S_\odot$ = (959.95 ± 0.05)″ for the value of the eclipse solar radius at 1 au, with negligible wavelength dependency.

Introduction

The eclipse solar radius is the radius to be used in very precise computations that predict the internal contact times of solar eclipses to a high level of accuracy. In particular, this is the radius that attempts to best reproduce the visual experience of a total solar eclipse. Such a solar radius corresponds closely with the notion of complete photospheric extinction.

Our methodology to estimate the eclipse solar radius relies on three components:

- Observing from the edge of the eclipse umbral shadow path
- Video recording of the flash spectrum
- Fitting synthetic light curves onto the observed ones

Observing full-silhouetted solar eclipses from the edge of the path to measure the solar radius [1] has been mainly pioneered by IOTA since the early '70s and provides some unique opportunities: all transient phenomena are extended and the sensitivity of several eclipse observables to the value of the solar radius gets greatly enhanced. As an example, Figure 1 depicts the sensitivity on the solar radius of the duration of totality for a location just a few hundred metres within the edge of the umbral shadow path and for a corresponding location on the centreline where mid-eclipse happens at the same time. While the duration on the centreline changes by only a couple of seconds when the value of the solar radius is increased from its traditional value (Auwers' value: 959.63″) to one more in line with experimental evidence (i.e. 960″), the duration varies considerably more for a location very near the edge.

In the 70s and 80s the Japanese Hydrographic Department recorded flash spectrum videos during several total solar eclipses with the aim, among others, to estimate the value of the solar

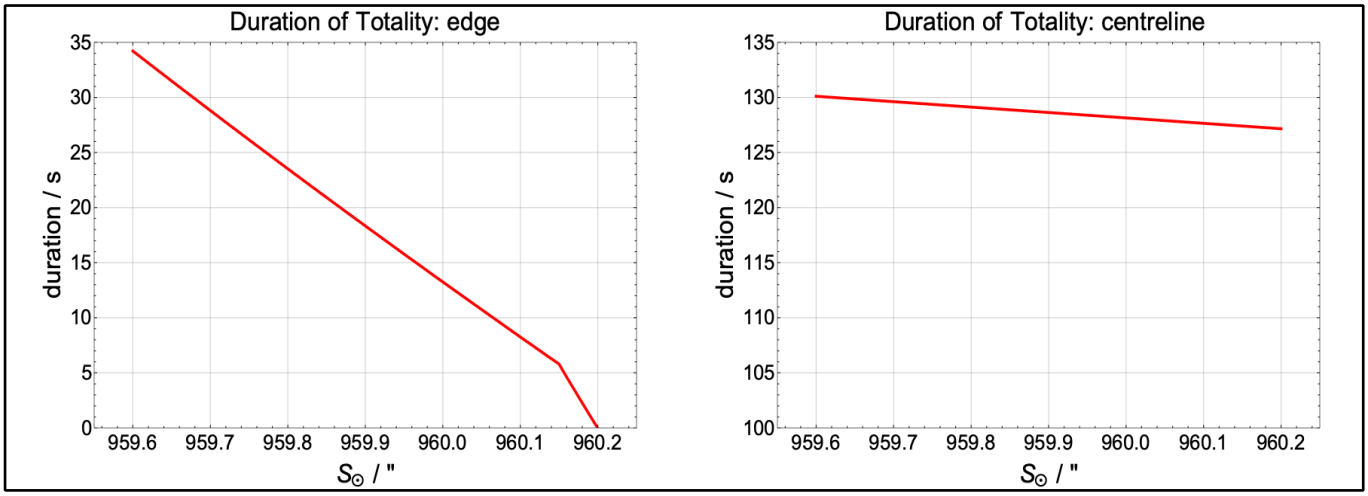

Figure 1. Sensitivity on the value of the eclipse solar radius $S_\odot$ at 1 au of the computed duration of totality for a location at the very edge of the umbral shadow path and for a corresponding location on the centreline. Data are for the 2017 August 21 total solar eclipse near the Oregon-Idaho border.

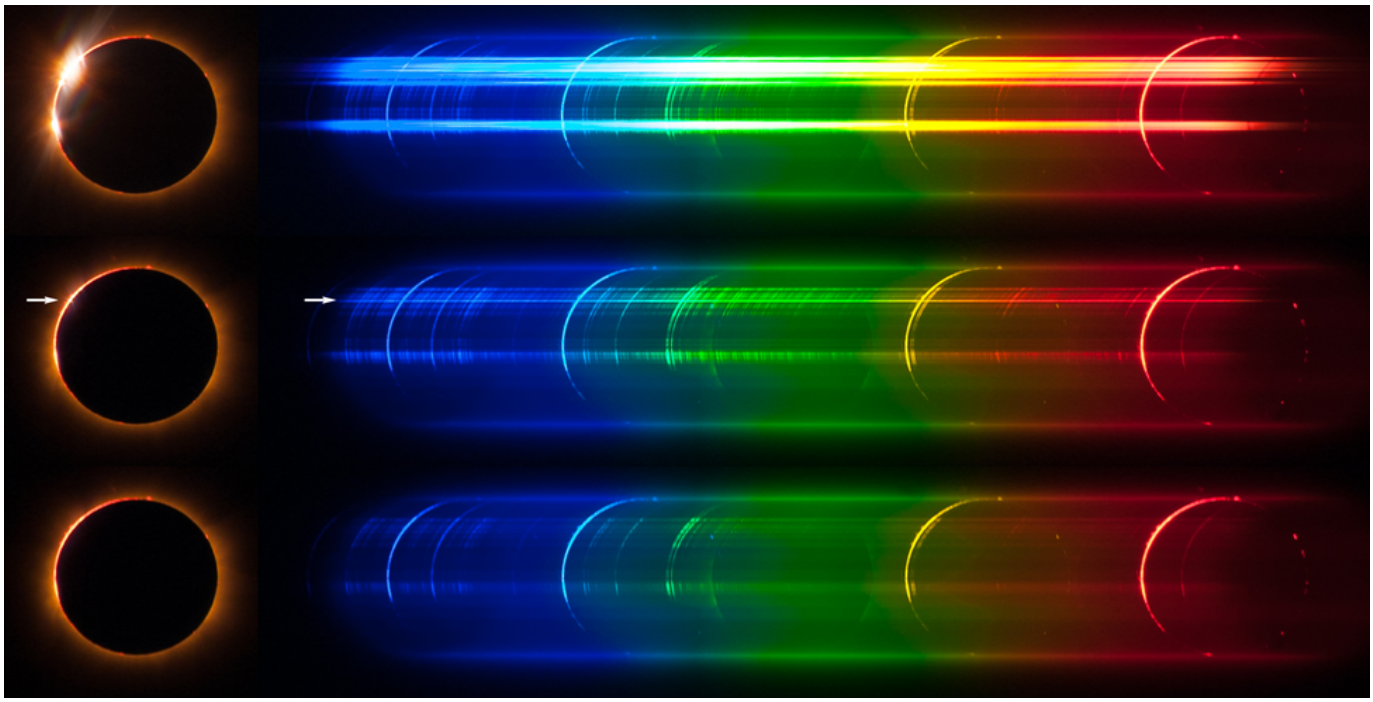

Figure 2. Example of the evolution of the flash spectrum at the onset of totality. On the left, white-light images of the eclipse showing the disappearing Baily's beads, the chromosphere and hints of inner corona. On the right, the corresponding spectra, revealing finer details. White arrows indicate the last vanishing Baily's bead and its photospheric continuum. The image is a composite but each pair white-light/spectrum was recorded on the same image. Data collected during the 2013 November 3 annular-total solar eclipse in Gabon using a Canon 5D Mark 1 with a 200 mm f/4 lens and a 100 lines/mm diffraction grating. (Credit: K. Emmanouilidis).

radius [2]. The flash spectrum is the (usually) fast evolving spectrum that can be observed at the onset and at the end of totality. It provides a detailed view of the light coming from the solar atmosphere and from the remnants of the photosphere. As an example, Figure 2 shows a sequence of composite images of a total solar eclipse just before and just after second contact and of the corresponding spectra. Baily's beads produce intense bands of continuum, the chromosphere generates characteristic arcs (mainly due to emission by Hydrogen, Helium, Magnesium and Sodium), the very lowest layers of the solar atmosphere produce a forest of very faint thin emission lines and the inner corona generates a mixed spectrum (a distinct round-shaped halo is seen in the green and it is due to Fe^{13+}).

Lamy's group has designed a method to estimate the value of the solar radius by collecting light curves with photometers just before second contact (C2) and just after third contact (C3) and by fitting synthetic light curves onto them [3]. Fitting a whole light curve has the advantage of being more constraining than just fitting point measurements.

Our methodology combines these three components: the enhanced sensitivity gained by observing from the very edge of the umbral shadow path, the wealth of information provided by the flash spectrum and the advantage obtained by fitting a whole curve of data points.

Method

The video of the flash spectrum was recorded using a Canon EOS 6D digital camera with a Canon EF 70–200 mm f/4L USM lens. The focus and the exposure were both set to manual and we chose an exposure time of 1/60s at an ISO setting of 100. A transmission diffraction grating, etched with 235 lines/mm, was mounted in front of the lens to separate the eclipse light into its spectral components.

The orientation of the diffraction grating is a critical aspect of the measurement, as it determines where the spectrum of the light coming from the Baily's beads will form within the width of the flash spectrum. As much as possible, as seen in Figure 3, the continuum of the Baily's beads should be towards the centre of the flash spectrum to enhance the separation of the individual beads. Because of the observing location being so close to the edge of the umbral shadow path, both the Baily's beads before C2 and after C3 form in the same neighbourhood of the lunar limb. It is then a matter of compromise to orientate the diffraction grating to image all Baily's beads well. In the example shown in Figure 3, the orientation is satisfying for the Baily's beads before C2, less optimal for the Baily's beads after C3. To facilitate the task of orientating the diffraction grating, the grating is housed within a threaded metallic ring that is screwed in front of the lens. The ring is only partially screwed into the lens thread before manually setting the spectrum into focus, a couple of minutes before C2. Once the spectrum is in focus, an adjustment to the orientation of the dif-

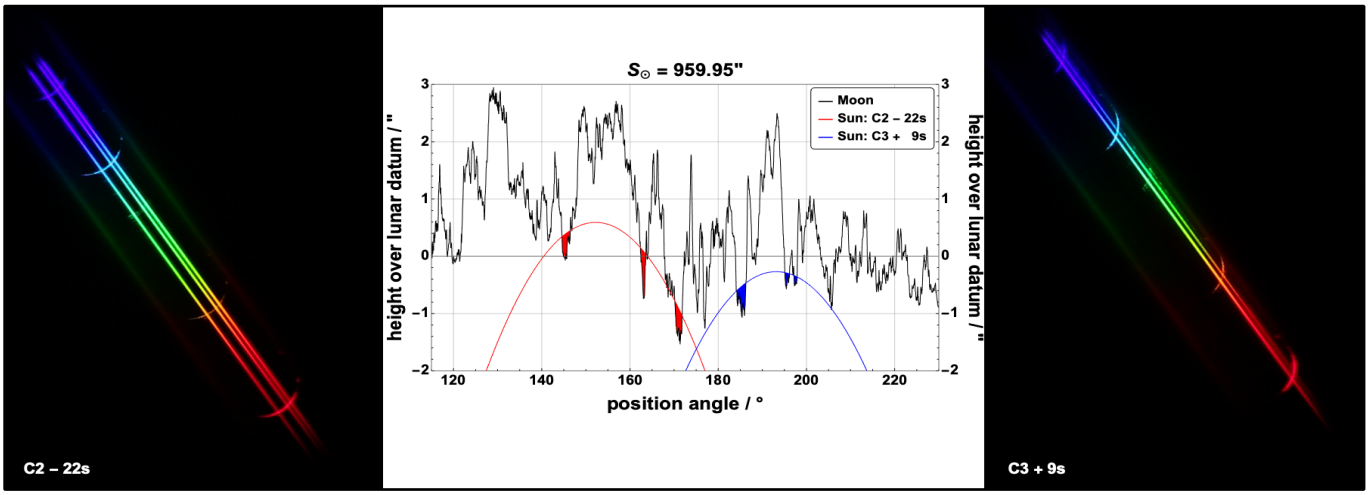

Figure 3. On the left and on the right, shape of the flash spectrum 22 s before C2 and 9 s after C3. In the centre, simulation of the mutual position of lunar and solar limb identifying the lunar valleys where the Baily's beads occur.

fraction grating can easily be performed, as there is leeway to rotate the metallic ring, to achieve the compromise explained above.

The light curves corresponding to a specific Baily's bead are extracted from the video of the flash spectrum by considering a small region of pixels in line with the continuum generated by the Baily's bead. To avoid contamination from neighbouring beads, we limited the analysis to the last bead before C2 and to the first bead after C3, as they usually persist isolated and alone for quite a few seconds. To eliminate as much light from the chromosphere as possible, the spectral regions where the light curves are extracted are chosen to be away from the main Hydrogen, Helium, Magnesium and Sodium emission lines. Another issue to consider is that the spectrum of the mesosphere (the first few hundred kilometres of the solar atmosphere) is superposed on the spectrum of the photosphere. As Figure 2 shows, a forest of faint lines always intersect the remaining continuum of the Baily's bead. To reduce the effect of these lines, the light curves are extracted from areas where the mesosphere is "quieter". The video is stored in such a way that a non-linear transformation (gamma correction) is applied to the linear output of the CMOS sensor of the DSLR camera. As we are interested in extracting light curves, that is to say, to perform relative photometry, we need to reverse this non-linear transformation to obtain the linear luminance, before averaging the signal over the pixels region.

The eclipse computational model relies on the latest ephemerides and accounts in a very precise way for all the complexity of the lunar topography and of the orientation of the celestial and terrestrial reference systems via robust algorithms and procedures. The model does not depend, like the traditional method, on Besselian elements to compute nominal predictions and then on applying limb corrections to account for the Moon's topography. Instead, it performs its computations directly with the solar limb and the lunar limb profile to find times of contact and other related quantities. No approximating adjustments are involved with these computations.

The simulated light curves are computed by integrating the limb darkening function over the exposed area of the photosphere (within a specific lunar valley) as depicted in Figure 4. The limb darkening function (LDF) describes the change in intensity of photospheric light by going from the centre of the Sun's disc to its periphery. The LDF also depends on wavelength [4]. The precise computational eclipse model is relied upon to describe the relative topocentric motion of the Sun's centre with respect to the Moon's centre, the evolving topocentric radii of the Moon's datum and of the Sun (based on the chosen value of the solar radius $S_\odot$ at 1 au), and the topocentric view of the topography of the lunar limb. The integration region R changes with time and it has a rather complex boundary.

Several adjustments are needed to fit the synthetic light curves over the observed light curves. Because the video recording does not have a UTC timestamp but just the relative timing among frames given by the framerate and because the simulations are naturally expressed using a UTC time base, a global time translation of the observed light curves needs to be applied before attempting a fit. Because the limb darkening function intensity is normalised and the observed light curves are expressed in arbitrary units, we need to apply a multiplicative scaling factor to the synthetic light curves to be able to perform the comparison with the observed light curves. The observed light curves do not go exactly to zero during totality due to several factors like the presence of diffuse background light and of residual light coming from the lowermost layers of the solar atmosphere. To account for this, a small bias is added to the synthetic light curves. We could alternatively subtract this bias from the observed light curves.

Even if the observed light curves from the Baily's bead before C2 and the Baily's bead after C3 are independent measurements, we constrained the fitting procedure to use the same time-shift, scaling factor and bias factor for both.

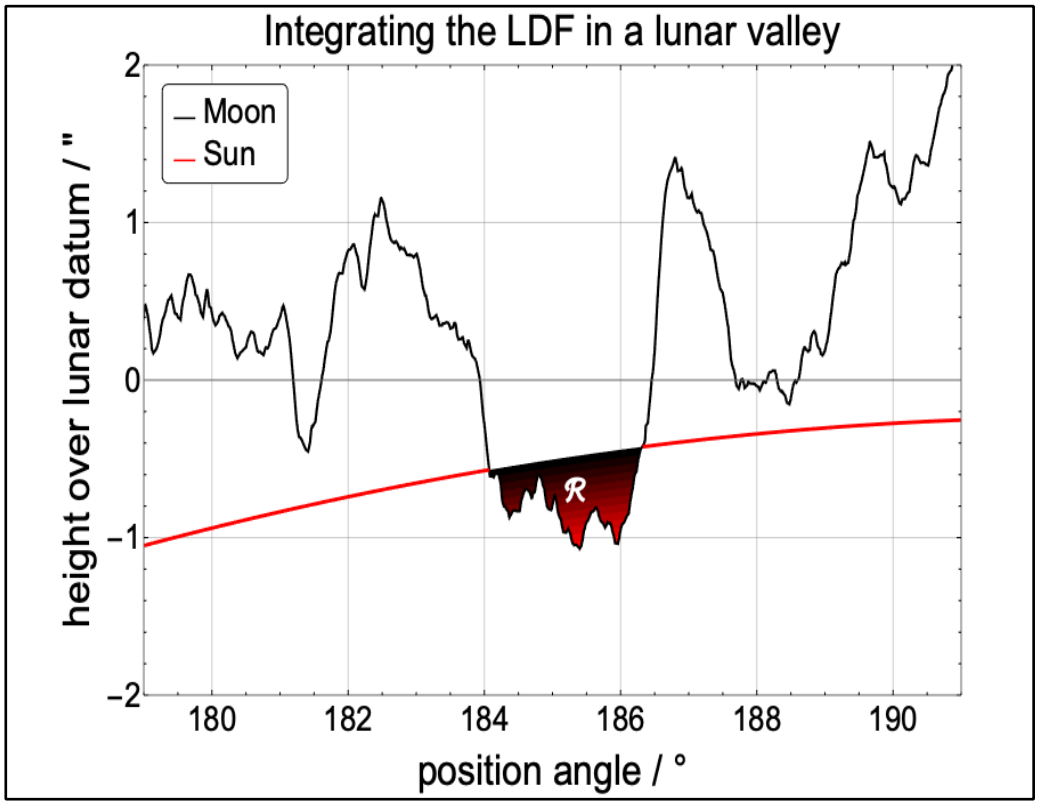

Figure 4. Synthetic light curves are generated by computing the integral of the limb darkening function over the exposed area of photosphere within the lunar valley generating the Baily's bead. The integration region R changes through time due to the relative movement of the solar and lunar limbs.

Observations

The observing location was south of Vale, Oregon, just a couple of hundred metres within the southern limit of the umbral shadow path. Its WGS84 geodetic coordinates are: λ = 117° 13′ 09.8″ W, φ = 43° 57′ 10.9″ N, h = 711 m. The landscape was very arid and the sky was cloudless. There were traces of smoke from forest fires but they were mainly towards the north and the west and they were never an issue.

The flash spectrum video we recorded can be seen following this link:

https://www.youtube.com/watch?v=eTqblNG-BHw

The video shows the slow evolution of the flash spectrum, mainly the disappearance and the reappearance of the photospheric continuum of several Baily's beads before second contact (C2) and after third contact (C3) with a brief period of totality in between. Figure 3 shows examples of the shape of the flash spectrum on the lead up to C2 and just after C3 and which lunar valleys generate the distinct thin bands of photospheric continuum.

If we focus on the duration of photospheric extinction, visual inspection of the video points to a duration no longer than 20 s, and possibly closer to 15 s. By referring to Figure 1, these durations of totality are quite incompatible with Auwers' solar radius (959.63″) and more indicative of a higher value, towards 960″.

Results

The analysis of the flash spectrum video proceeds in several steps: extracting the light curves (from a narrow spectral region) of the last Baily's bead before C2 and of the first Baily's bead after C3, simulating synthetic light curves by integrating the limb darkening function in the lunar valleys that generate the Baily's beads, fitting the solar radius $S_\odot$ to get the best agreement between the synthetic light curves and the observed light curves. The solar radius $S_\odot$ at 1 au directly determines the topocentric solar radius $\Sigma_\odot$ that is considered as the free parameter in the functional form of the limb darkening function.

Figure 5 shows the observed light curves (extracted from a spectral region around 580 nm, near the main Helium line) together with the synthetic light curves generated for three different values of the solar radius $S_\odot$. The best agreement is achieved when $S_\odot$ = 959.95″. The other simulations provide an idea of the uncertainty of this estimate. Conservatively, we can say that the final estimate of the solar radius (at around 580 nm) is: $S_\odot$ = 959.95 ± 0.05)″. An important remark is that identical values for the multiplicative scaling factor and bias were used for the synthetic light curves when different values of the assumed solar radius $S_\odot$ were used to define the limb darkening function. It is important to clamp down on the degrees of freedom we can play with.

We repeated the fitting procedure for other spectral regions, namely 480 nm (near the *H*β line) and 640 nm (near the *H*α line).

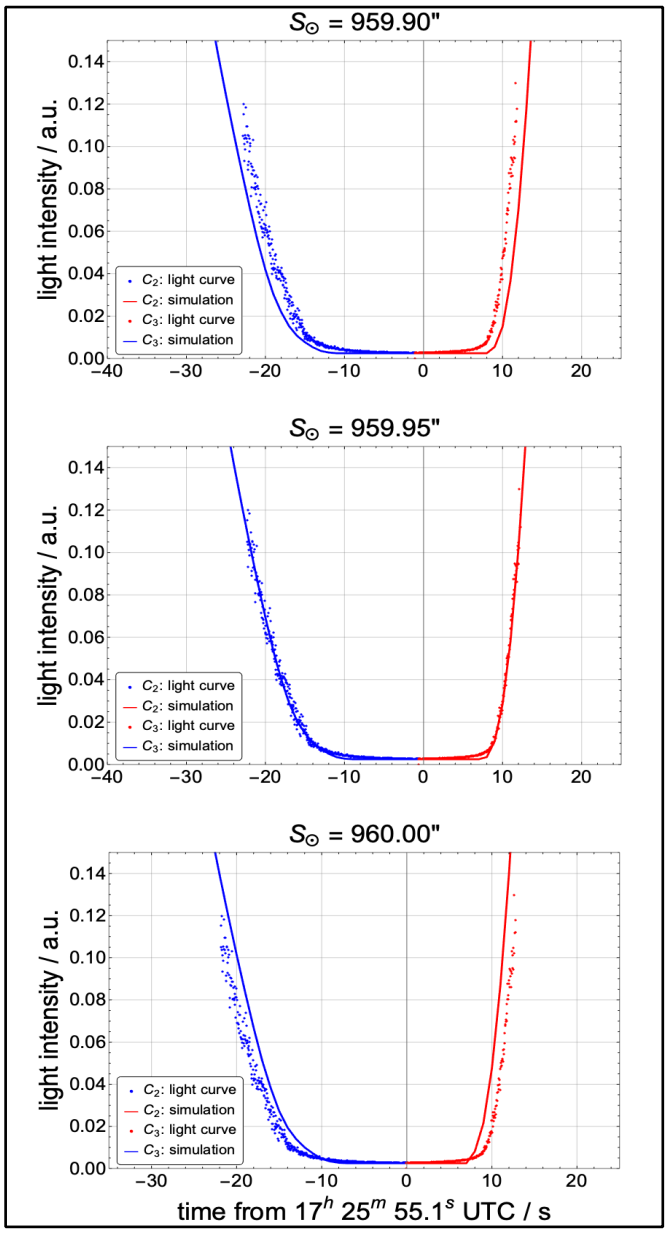

Figure 5. Fit of synthetic light curves onto observed light curves, extracted around 580nm, for various values of the solar radius $S_\odot$.

Figure 6 shows that the estimated value of the solar radius is quite similar at different wavelengths, well within the uncertainty of the measurement. Models predict the solar radius to be different at different wavelengths [5], but the difference is computed to be of the order of 0.02″ by going from the blue to the red part of the spectrum, too small to be conclusively detected by the sensitivity of our estimation.

While performing these fits at different wavelengths, different values for the scaling factor and bias for the synthetic light curves had to be used. This is due to the fact that the spectral response of the CMOS sensor is not flat and changes depending on the wavelength of the light impacting on it. So the same scaling parameters cannot work at very different wavelengths.

Discussion

The estimate of the eclipse solar radius we have obtained $S_\odot$ = (959.95 ± 0.05)″ is larger than the traditional standard value $S_\odot$ = 959.63″ still used in most published eclipse predictions and it is in line with a growing body of measurements collected in the recent past during total solar eclipses [3].

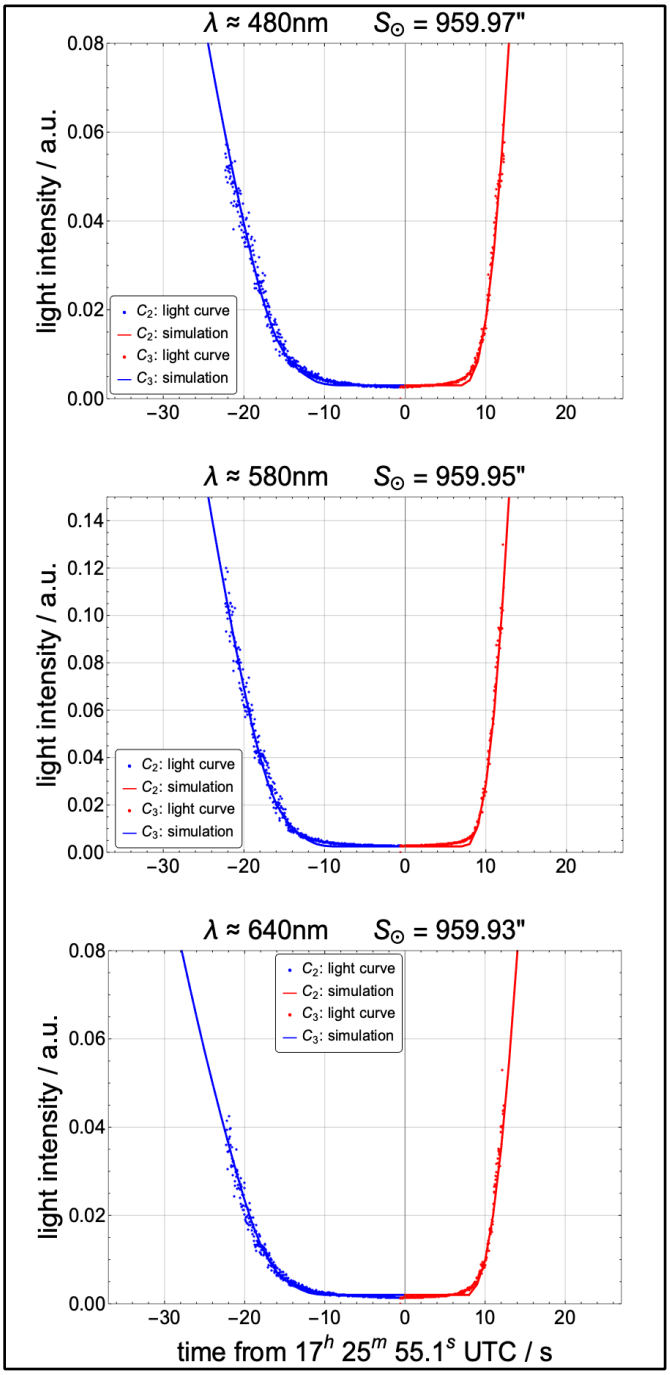

Figure 6. Best fit of synthetic light curves onto observed light curves, at different wavelengths.

The flash spectrum video we collected did not have UTC timestamping associated with it, but we can estimate post-facto the UTC time of each frame as a by-product of the fitting procedure. This allows comparing side-by-side the evolution of the flash spectrum and the simulation of the relative movement of the solar limb with respect to the lunar limb. These comparisons can be found here:

https://www.youtube.com/watch?v=JI2AIRI9Prk
https://www.youtube.com/watch?v=LTxSM4Goo5A

As we expect, the simulation computed assuming $S_\odot$ = 959.95" reproduces the timing of disappearance and reappearance of the photospheric continuum of the various Baily's beads far better than the one obtained by assuming the standard radius $S_\odot$ = 959.63".

The methodology we have used to construct synthetic light curves implicitly assumes that the photosphere ends sharply and it is the sole contributor to the observed light curves. By choosing suitable spectral regions where the light curve measurements are performed, we can eliminate any contribution of the medium-high chromosphere and minimise the contribution from the mesosphere. We believe that, as we are fitting a whole light curve, the impact of the mesosphere is lessened. It is also partly compensated by the bias factor. We can nevertheless observe some minor discrepancies at third contact between synthetic and observed light curves.

Conclusion

We estimated the value of the eclipse solar radius at 1 au during the 2017 August 21 total solar eclipse to be $S_\odot$ = (959.95 ± 0.05)" at around 580 nm, with little variation across different wavelengths. The estimation methodology relies on recording a flash spectrum video from the very edge of the umbral shadow path and on computing synthetic light curves by integrating the limb darkening function over the exposed area of photosphere.

Our measurement is a contribution to the wider effort aimed at measuring the solar radius during full-silhouetted solar eclipses. Its goals are both to provide better input data for eclipse computational models, and improving their accuracy, and to provide data for the long term monitoring of the variability of the solar radius.

Future Plans

We aim to repeat these measurements during the 2023 annular-total eclipse and to improve the way data are collected. Two major improvements will come by collecting raw data and by adding UTC time-stamping to the video recording.

Having access to raw data from the imaging sensor will remove the need to undo any transformations that were applied to the sensor data and will allow performing more accurate relative photometry. Even if we can perform the fitting procedure without relying on UTC time-stamping, having time-stamping would eliminate a degree of freedom in the methodology and make it more constraining and robust. UTC time-stamping of the flash spectrum observations would also likely open up the possibility to investigate the accuracy of eclipse computational models [6] (see Appendix C). We are looking at using the QHY-174M GPS CMOS camera to achieve these two goals.

References

[1] Guhl K., *Baily's Beads Observations during the Total Solar Eclipse 2019 July 2*, Journal for Occultation Astronomy, vol. 10, no. 2, pp. 3-7 (2020) https://www.iota-es.de/JOA/JOA2020_2.pdf

[2] Kubo Y., *Position and Radius of the Sun Determined by Solar Eclipses in Combination with Lunar Occultations*, Publications of the Astronomical Association of Japan, vol. 45, pp. 819-829 (1993) https://articles.adsabs.harvard.edu/pdf/1993pasj...45..819k

[3] Lamy P. et al., *A Novel Technique for Measuring the Solar Radius from Eclipse Light Curves - Results for 2010, 2012, 2013 and 2015*, Solar Physics, vol. 290, pp. 2617-2648 (2015) https://link.springer.com/content/pdf/10.1007/s11207-015-0787-8.pdf

[4] Hestroffer D. & Magnan D., *Wavelength Dependency of the Solar Limb Darkening*, Astronomy and Astrophysics, vol. 333, pp. 338-342 (1998)
http://aa.springer.de/papers/8333001/2300338.pdf

[5] Raponi A. et al., *The Measurement of Solar Diameter and Limb Darkening Function with the Eclipse Observations*, Solar Physics, vol. 278, pp. 269-283 (2012)
https://link.springer.com/content/ pdf/10.1007/s11207-012-9947-2.pdf

Further Reading

[6] Quaglia L. et al., *Estimation of the Eclipse Solar Radius by Flash Spectrum Video Analysis*, The Astrophysical Journal Supplement Series, vol. 256, article 36 (2021)
https://iopscience.iop.org/article/10.3847/1538-4365/ac1279

Journal for Occultation Astronomy

The First PHEMU Campaign in 1908

Konrad Guhl · IOTA/ES · Berlin · Germany · kguhl@astw.de

ABSTRACT: The observation of mutual phenomena of Jovian satellites in the PHEMU campaigns have been known since 1973. Research on such observations in the pre-internet era showed that, after random observations in the 19th century, the first international campaign on such events took place as early as 1908. The predictions published by Oudemans in 1906 were the basis for 11 observers from several countries to observe systematically. In the paper 17 observed events are compared with the modern simulation. The mean value of the O-C value of the visual observations of the campaign is -0.15 minutes.

Introduction

Since 1973, the mutual phenomena of Jovian satellites have been systematically predicted, observed and the results evaluated. The French astronomer J.E. Arlot has planned, managed and evaluated the observation campaigns since then. He also introduced the term PHEMU as an abbreviation of "phénomènes mutuels". The observations obtained are accessible in the "Natural Satellites Data Center".

Of course, such events, for which the name PHEMU will be used in the following, also took place before 1973. The author has been searching for observation reports (all evaluated observations are listed in Table 1) from the "pre-Internet time" in the literature for a long time and presents first results here. The oldest mention of such phenomena dates from the time of the discovery of Jupiter's moons: Simon Marius, who discovered Jupiter's moons independently of Galileo Galilei, observed them regularly and frequently.

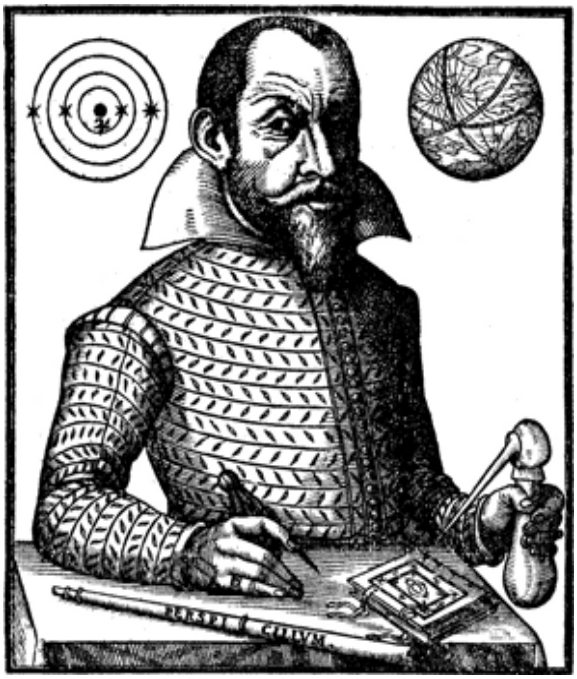

Figure 1. Simon Marius (1573 – 1624), (credit: Simag-ev)

He reports a perception of Jupiter's moon IV as darker than usual. Marius explains this with a shadow (eclipse) cast by Moon II or III [1]. This observation is dated 1613 February 17.

A check by N. Emelyanov of the Sternberg Astronomical Institute (SAI) in Moscow unfortunately revealed no such event for that day [2]. The conclusion that mutual eclipses of satellites are possible, published in [1], 1614 is an erratic conclusion for that time.

Early Observations

The first documented observation was made by the German amateur astronomer Ch. Arnold in 1693. Christian Arnold (1650-1695) was a farmer in Sommerfeld, a village near Leipzig. He observed, among other things, the comet Halley, a Mercury transit and also Jupiter moon occultations or eclipses. Secondary literature [3] reports that Arnold saw the occultation of moon II by III. This observation of 1.11.1693, as well as the observations of Luthmer [4] and [5] of 1819, 1820 and 1822, happened to be made during Jupiter's satellites observations. Both Arnold and Luthmer knew of their rarity and therefore published them. An analysis of these observations with the IMCCE Internet program MULTISAT [21] showed that they were very close conjunctions that could not be resolved with the instruments of the time.

First Analyses

In the 2nd half of the 19th century more attention was paid to the observations of Jupiter's satellite phenomena and also a PHEMU was noticed: The observation of F. Jackson [6] was evaluated and discussed by A.C.D. Crommelin in [7] with the help of Mr. Marth: The graphics from [7] are reproduced in Figure 2.

Crommelin came to the following conclusion: "*It will be seen that an error of 2" in the difference of the latitudes of the satellites, as given by the Tables, would suffice to bring II partially within the penumbra of III. Such an error is larger than we should expect, but perhaps not wholly inadmissible. I am, however, by no means confident that an eclipse actually occurred; though, if not, the almost perfect agreement in time between this observation and conjunction with the shadow would be curious coincidence.*"

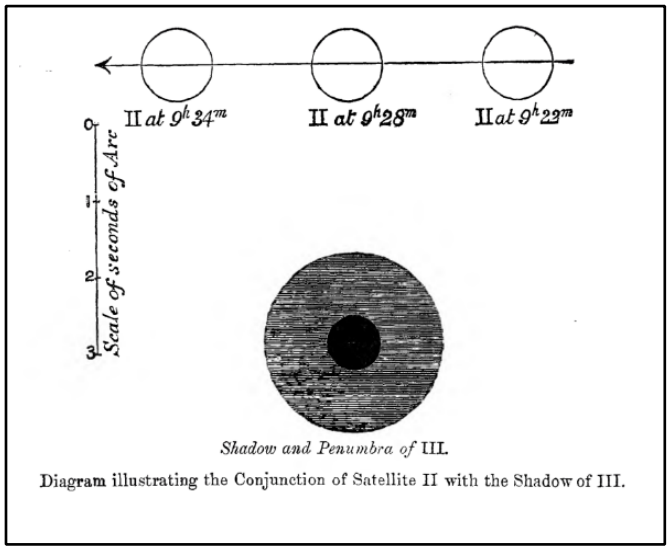

Figure 2. Simulation following analysis from Crommelin [7]

Crommelin's doubts are justified, no PHEMU event could be found by the author for the observation.

Nijland calculated the diameters of the moons from the duration of the occultation of Ganymede (III) by Europa (II) on 1902 July 16 [11]. He calculated the sum of both diameters to be 2.38" from the observed duration of the occultation of 10m20s = 0.172 h and the relative motion of 13.86"/h. This is in excellent agreement with the values known at the time of 0.87" for Europa and 1.51" for Ganymede.

The First PHEMU Campaign

The moon and planet observer Ph. Fauth (1867-1941) wrote after first, accidental observations [9] of PHEMUS in 1902 and 1903: *"It must be possible to obtain from exact tracing of the mutual occultation of two moons... the most accurate test of the orbital elements..."*[8]

He called for ephemerides and observations for the time of the next equinox on Jupiter. Thus, the value of observations, the precise determination of orbits, was recognised!

The ephemerides for the coming equinox in 1908 were then calculated and published by J. A. C. Oudemans [10]. Jean Abraham Chrétien Oudemans was a Dutch astronomer. In his long life as a scientist and explorer he spent 18 years in the Dutch Indies. There he conducted extensive geodetic operations and published his work on the triangulation of the island of Java (today: Jawa, Indonesia) in six volumes. On 1874 December 9, he and his expedition members observed a transit of Venus from Reunion Island. Oudemans retired in 1898 and continued to be engaged in astronomical and geodetic work.

In his introduction to [10] he explicitly refers to Fauth's request. He reports and analyses all PHEMU observations known to him (observations 1, 5-8, 10,11, 13-16 in Table 1) and calculates 72 geocentric conjunctions for the months of June and July 1908 for the prediction of mutual eclipses. Furthermore, he publishes 81 heliocentric conjunctions for possible mutual eclipses for April

Figure 3. J. A. C. Oudemans (credit: Wikipedia, public)

and May of that year. The observers Kostinsky (Pulkovo, Russia), Pidoux (Geneva, Switzerland), Innes (Johannesburg, South Africa) and Whitmell (Leeds, UK) refer to these predictions in their reports. For the other observations of 1908, it can be assumed that Oudeman's prediction was the basis. Oudemans did not live to see the success of his ephemeris - he died in December 1906. The author found 26 observational results obtained in this campaign (no. 18-43, Table 1). When comparing the observations with the simulations, the following discrepancies arise in the 1908 campaign:

- **Whitmell:**

No simulation could be found for the reported event.

- **Phillips:**

The observer reports in [15] as observation time 28.03.1908 12h00 to 12h07 Greenwich time. In this time the European observers had the day begin at noon to avoid the date change at night. The observation is therefore 29.03.1908 00h00 to 00h07. Phillips reports he observed the PHEMU IIOI. Such an event is to be simulated for 29.03.1908 from 01h01m06s to 01h06m 57s [21]. Since the event and minute fit, an error in the hour is assumed.

- **Innes:**

In observation No. 30, Innes observes at the right time, but fails to notice a 0.45 mag drop in brightness.

- **Milowanow and Khowanski:**

Observations no. 37 and 38 do not belong to the phenomenon Io eclipses Callisto (IEIV), as reported in [12]. This event only had a brightness drop of 0.09mag. The two observers observed the eclipse of Callisto by Europa (IIEIV) in which the brightness drop during total phase was 0.512mag. Curiously: The event IIEIV is explicitly described as having been observed but not registered by Milovanov (observation no. 39).

- **Pidoux:**

The observed events are predicted by Oudemans but they do not fit into any simulation according to [21].

No.	Date YYYY MM DD	Time	Event	Simulation Event (UT) YYYY MM DD HH MM SS – HH MM SS	Observer	Source
1	1693 11 01	10h47m local	IIIOII	Close conjunction	Arnold	[3]
2	1819 08 22	11h10m local	IOII (?)	Close conjunction	Luthmer	[4]
3	1820 11 12	From 07h00m local	IIOI	No result	Luthmer	[4]
4	1820 12 20	05h30m local	IIOIII	Close conjunction	Luthmer	[4]
5	1822 10 30	6h55m	IIIOIV	No result	Luthmer	[5]
6	1885 03 27	12h20m	IIIOI	Close conjunction	Williams	[10]
7	1891 08 14	23h49m - 23h59m	IIEI	1891 8 14 23 21 28 - 23 49 47 2E1	Comas Solà	[10]
8	1891 08 15	00h00m - 00h04m	IIEI	1891 8 14 23 21 28 - 23 49 47 2E1	Williams	[10]
9	1896 03 30	21h20m	IIIEII	No result	Jackson	[7]
10	1902 07 16	01h52m	IIOIII	1902 7 16 1 49 53 - 1 59 30 2O3	Williams	[10]
11	1902 07 16	01h54m50s	IIOIII	1902 7 16 1 49 53 - 1 59 30 2O3	Nijland	[11]
12	1902 09 03	21h51.5m	IIOIII	1902 9 3 21 48 5 - 21 54 10 2O3	Worthington	[20]
13	1902 10 07	20h16m	IIOI	1902 10 7 20 13 38 - 20 18 9 1O2	Fauth	[8]
14	1902 10 23	19h07m03.5s	IIOIII	1902 10 23 19 5 19 - 19 9 10 2O3	Fauth	[8]
15	1902 11 10	18h33m20s	IIIOI	1902 11 10 18 29 52 - 18 37 42 3O1	Fauth	[8]
16	1902 12 24	17h24m30s	IOIV	1902 12 24 17 22 4 - 17 27 59 1O4	Fauth	[8]
17	1903 01 14	17h02m (start)	IIIOII	1903 1 14 17 12 35 - 17 32 32 3O2	Fauth	[8]
18	1908 01 24	00h51m +/- 5s	IOII	1908 1 23 23 49 35 - 23 53 56 1O2	Fauth	[6]
19	1908 01 25	22h05m first contact	IIOIII	No result	Whitmell	[14]
20	1908 02 20	19h17m55s	IIIOIIP	1908 2 20 19 15 50 - 19 20 46 3O2	Fauth	[18]
21	1908 02 20	19h15m06s - 19h20m55s	IIIOIIP	1908 2 20 19 15 50 - 19 20 46 3O2	Knopf	[18]
22	1908 02 24	20h44.2m	IOII	1908 2 24 20 43 50 - 20 47 23 1O2	Kostinsky	[17]
23	1908 02 24	20h45m32s	IOII	1908 2 24 20 43 50 - 20 47 23 1O2	Hartmann	[19]
24	1908 02 24	20h45m23s	IOII	1908 2 24 20 43 50 - 20 47 23 1O2	Innes	[16]
25	1908 02 27	22m05m59s	IIIOII	1908 2 27 22 4 7 - 22 7 48 3O2	Innes	[16]
26	1908 03 14	20h43.8m	IIOI	1908 3 14 20 40 36 - 20 45 56 2O1	Phillips	[15]
27	1908 03 21	22h52m	IIOI	1908 3 21 22 49 36 - 22 55 10 2O1	Phillips	[15]
28	1908 03 29	00h03.8m	IIOI	1908 3 29 1 1 6 - 1 6 57 2O1	Phillips	[15]
29	1908 04 03	21h51.0m	IEIIP	1908 4 3 21 49 14 - 21 53 27 1E2	Kostinsky	[17]
30	1908 04 03	No dimming from 21h40m to 22h	IEII	1908 4 3 21 49 14 - 21 53 27 1E2	Innes	[16]
31	1908 04 08	18h25m52s	IIEI	No result	Milowanow	[12]
32	1908 04 08	No dimming	IIEI	No result	Innes	[16]
33	1908 04 08	16h26m29s	IIOI	1908 4 8 16 23 49 - 16 30 9 2O1	Innes	[16]
34	1908 04 15	18h46m18.4s	IIOI	1908 4 15 18 42 42 - 18 49 26 2O1	Innes	[16]
35	1908 04 22	21h07m20s	IIOI	1908 4 22 21 5 6 - 21 12 17 2O1	Baranow	[12]
36	1908 05 05	Observed, nothing notice	IEIII	1908 5 5 19 8 25 - 19 15 11 1E3	Milowanov	[12]
37	1908 05 07	18h37m03s	IEIV	1908 5 7 18 26 0 - 18 32 15 1E4	Milowanov	[12]
38	1908 05 07	18h37m43s	IEIV	1908 5 7 18 26 0 - 18 32 15 1E4	Khowanski	[12]
39	1908 05 07	Observed, not notice	IIEIV	1908 5 7 18 33 1 - 18 42 46 2E4	Milowanow	[12]
40	1908 05 08	19h03m16s	IIIEIV	No result	Milowanov	[12]
41	1908 06 01	18h10m19s	IIOI	1908 6 1 18 3 33 - 18 16 9 2O1	Innes	[16]
42	1908 06 17	20h32m GMT	IIOIV	20h38m by Oudemans	Pidoux	[13]
43	1908 07 03	19h52m GMT	IIIOIV	19h58.5m by Oudemans	Pidoux	[13]

Table 1. Historical observations up to 1908

Remarks for Table 1:
Unless otherwise stated, the times given in the third column of the table are converted to longitude 0° (GMAT - Greenwich Mean Astronomical Time) from the zone time or local time given by the observer. The events are uniformly designated O for Occultation or E for Eclipse. IEIII means moon I eclipses moon III. Where possible, the simulation has been calculated with [21]. Where this software did not find an event, it is assessed whether the observation can be explained by a close conjunction or whether there is a prediction by Oudemans [10]. If no close conjunction or phenomena of the moons could be found at the time of observation, "No result" is entered.

Accuracy of the Visual Observations

For further evaluation, the above-mentioned unclear observations are not considered further and the evaluated observations are listed in Table 2.

Tab 1 no.	Date YYYY MM DD	Observation time	Calculated time [21]	O-C in minutes	Observer
10	1902 07 16	01h52m	01h 53m48s	-1.8	Stanley Williams
11	1902 07 16	01h54m50s	01 h53m48s	+1.03	Nijland
12	1902 09 03	21h51.5m	21h51m07s	+0.38	Worthington
13	1902 10 07	20h16m	20h15m53s	+0.12	Fauth
14	1902 10 23	19h07m03.5s	19h07m44s	-0.67	Fauth
15	1902 11 10	18h33m20s	18h33m47s	-0.45	Fauth
16	1902 12 24	17h24m30s	17h25m02s	-0.53	Fauth
17	1903 01 14	17h02m (start)	17h12m35s	-9.42	Fauth
18	1908 01 23	23h51m +/- 5s	23h51m45s	-0.75	Fauth
20	1908 02 20	19h17m55s	19h18m17s	+0.91	Fauth
21	1908 02 20	19h17m36s	19h18m17s	+0.68	Knopf
22	1908 02 24	20h44.2m	20h45m57s	-1.75	Kostinsky
23	1908 02 24	20h45m32s +/- 5s	20h45m57s	-0.41	Hartmann
24	1908 02 24	20h45m23s	20h45m57s	-0.57	Innes
25	1908 02 27	22m05m59s	22h05m57s	0	Innes
26	1908 03 14	20h43.8m	20h43m26s	-0.37	Phillips
27	1908 03 21	22h52m	22h52m23s	-0.38	Phillips
28	1908 03 29	00h03.8m	01h04m06s	0.3	Phillips
29	1908 04 03	21h51.0m	21h51m21s	-0.35	Kostinsky
33	1908 04 08	16h26m29s	16h26m59s	-0.5	Innes
34	1908 04 15	18h46m18.4s	18h46m04s	0.24	Innes
35	1908 04 22	21h07m20s	21h08m42s	-1.34	Baranow
37	1908 05 07	18h37m03s	18h36m47s	+0.27	Milowanow
38	1908 05 07	18h37m43s	18h36m47s	+0.93	Khowanski
41	1908 06 01	18h10m19s	18h09m46s	0.55	Innes

Table 2. O-C for usable observations from Table 1

The mean value of the O-C value of the remaining 24 measured values is -0.55 min. An astonishingly low value that speaks for the care and skill of the observers of visual astronomy.

Of the 25 observations in Table 2, 17 were carried out in the "PHEMU08" campaign. The mean value for O-C for these observations is -0.15 min.

Conclusion

International campaigns in observational astronomy were also successfully carried out in the pre-internet age. Modern simulations allow us to check the accuracy of the above-mentioned observations and to determine the value of visual observations of this era on the basis of the low O-C values. This is an important indication for the evaluation of historical observations when no verifications are possible.

Acknowledgements

The author would like to thank the following libraries for their help:

Archenhold Sternwarte, Berlin
Leibnitz Institute for Astrophysics, Potsdam
Ghent University, Ghent
Sternwarte Bergedorf, Hamburg
For the research in the UK, I thank Alex Pratt, Leeds.

References

[1] Marius, S., Mundus Iovialis – Die Welt des Jupiter, edited by Joachim Schlör, Reihe Fränkische Geschichte, Bd. 4, Gunzenhausen: Schrenk, 1988
[2] e-mail communication Nicolai Emelyanov – Konrad Guhl
[3] Houzeau, J.-C., Vade-mecum de l'astronome, F. Hayez, Brüssel, 1882, P. 666
[4] Luthmer, D. J. J., Astronomische Beobachtungen, vom Herrn Prediger Luthmer in Hannover, unterm 9. August 1821 eingesandt, Berliner Astronomisches Jahrbuch 1824, P. 242, Berlin, 1821
[5] Luthmer, D. J. J., Astronomische Nachrichten, vom Prediger Luthmer in Hannover, unterm 3. Sept. 1823 eingesandt", Berliner Astronomisches Jahrbuch 1826 P. 224, Berlin, 1823
[6] Fauth, Ph., Trabantenphänomene Jupiters, Astronomische Nachrichten Vol. 177 (1908) P. 143, Kiel, 1908
[7] Crommelin, A. C. D., Notes on a Possible Eclipse of Jupiter's Second Satellite by the Shadow of the Third 1896 March 30, Monthly Notices of the Royal Astronomical Society, Vol. 56 (1896), P. 474
[8] Fauth, Ph., Seltene Konjunktionen im Jupitersystem, Astronomische Nachrichten Vol. 161 (1903) P. 102, Kiel 1903
[9] Fauth, Ph., Jupiterbeobachtungen während 35 Jahren, Leipzig, 1925
[10] Oudemans, J. A. C., Occultations et eclipses mutuelle des Satellites de Jupiter 1908, Utrecht, 1907
[11] Nijland, A. A., Konjunktion der Jupitermonde II und III, Astronomische Nachrichten Vol. 161 (1903) P. 307, Kiel 1903
[12] Baranow et al., Beobachtungen von Planeten, des Kometen 1908c (Morehouse) von Sternbedeckungen und von Jupiterstrabanten-Erscheinungen auf der kaiserlichen Universitätssternwarte zu Kasan, Astronomische Nachrichten Vol. 181 (1909) P. 49, Kiel, 1909
[13] Pidoux, F., Occultation mutelle des satellites II et IV de Jupiter le 17 Jun. 1908, Astronomische Nachrichten Vol.181 (1909) P.298, Kiel, 1909
[14] Whitmell, C. T., Moon occulting Moon, The Journal of the British Astronomical Association, Vol XVIII, P. 180-181, London, 1908
[15] Phillips, T. E. R., Observations of Jupiter during Apparition of 1907-8", Monthly Notices of the Royal Astronomical Society, Vol. 69 (1908), P. 38-38
[16] Innes, R. T. A., Observations of Jupiter's Galilean Satellites, January-June 1908, Monthly Notices of the Royal Astronomical Society, Vol. 69 (1908), pp. 512-534
[17] Kostinsky, S., Observations de quelques phenomenes interessants dans le systeme des Satellites de Jupiter, Astronomische Nachrichten Vol. 178 (1908) P. 14
[18] Fauth, Ph., Konjunktion des II. und III. Jupitermondes, Astronomische Nachrichten Vol. 178 (1908) P. 15, Kiel, 1908
[19] Fauth, Ph., Bedeckung des II. Jupitermondes durch den I. am 24. Februar 1908, Astronomische Nachrichten Vol. 178 (1908) P.119, Kiel, 1908
[20] Worthington, J. H., Mutual Occultations of Jupiter's Satellites, The Journal of the British Astronomical Association, Vol XIX, P. 95, London, 1909
[21] Simulation (Ephemeride: J1-J4 by Lainey et al. (2009) V2.0) used at http://nsdb.imcce.fr/multisat/nssphe0he.htm

Database:
http://nsdb.imcce.fr/obsphe/obsphe-en/fjuphemu.html

Further Reading

Arlot, J.-E., Emelyanov, N., The Campaign of Observation of the Mutual Occultations and Eclipses of the Galilean Satellites of Jupiter in 2021, Journal for Occultation Astronomy, No. 2020-04, pp. 3-10 https://www.iota-es.de/JOA/JOA2020_4.pdf

A Collaborative Research for Occultations by NEAs

ACROSS (Asteroid Collaborative Research via Occultation Systematic Survey) is built on a team of researchers and graduate students from Observatoire de la Côte d'Azur (OCA), France, and the Aristotle University of Thessaloniki (Auth), Greece, with the support of ESA.

The ACROSS Project is driven by the breakthroughs in occultations brought thanks to the *Gaia* catalogues. It is now possible to start planning on a consistent basis events by Near Earth Asteroids (NEA). We've already seen through the past few years campaigns featuring occultations by (3200) Phaethon and (99942) Apophis. The ACROSS project provides mainly support to the *Hera* mission targets. It will focus at first on the binary asteroid (65803) Didymos and other *Hera* flyby targets. It will nonetheless also include other NEAs.

More details can be found on the dedicated webpage https://lagrange.oca.eu/fr/home-across. To contact the team, please use the following address across@oca.eu.

Our Targets

The ACROSS team has defined 3 categories of targets, listed here by the ranking priority:

1. Didymos

The binary NEA (65803) Didymos is our main target throughout this project. It is the target of the first planetary defence programme through the missions *DART* (NASA) and *Hera* (ESA). The kinetic impactor *DART* will impact Dimorphos (Didymos' satellite) on 2022 September 26th at 23:14 UT, changing the mutual orbit of the system.

Our goal is to detect occultations by this system before and after impact, while keeping in mind that very good opportunities prior to impact are extremely rare. It should be stressed here that Didymos is a small asteroid (diameter of ~0.8 km), and therefore all of its events are sub-second in duration, with most having a maximum duration around 0.2 s. Therefore, it is required that any observer attempting these events has the equipment necessary to go down to these durations for the exposure time. Only occultation-derived astrometry will allow us to better assess the effect of the impactor on the heliocentric orbit. This new derived astrometry will also be important for the *Hera* mission.

2. Other *Hera* Targets

Hera is expected to be launched in 2024, on its way to Didymos it will fly by a couple of other secondary targets. So far, 9 targets have made it to the shortlist: (29886) Randytung, (42532) 1995 OR, (54212) 2000 HJ89, (88992) 2001 TJ72, (95802) Francismuir, (122764) 2000 SX69, (169549) 2002 EG105, (188708) 2005 TR99, and (477416) 2009 WW1.

3. Other NEAs

We have selected a list of other NEAs with a "good-enough" orbital solution to predict occultations with "reasonable" uncertainties for campaigns.

All our predictions will be available through our campaign page https://lagrange.oca.eu/fr/prediction, and via the *Occult Watcher Cloud* https://cloud.occultwatcher.net/events/tagged/ACROSS. The highest priority campaigns will also be advertised through the different mailing lists.

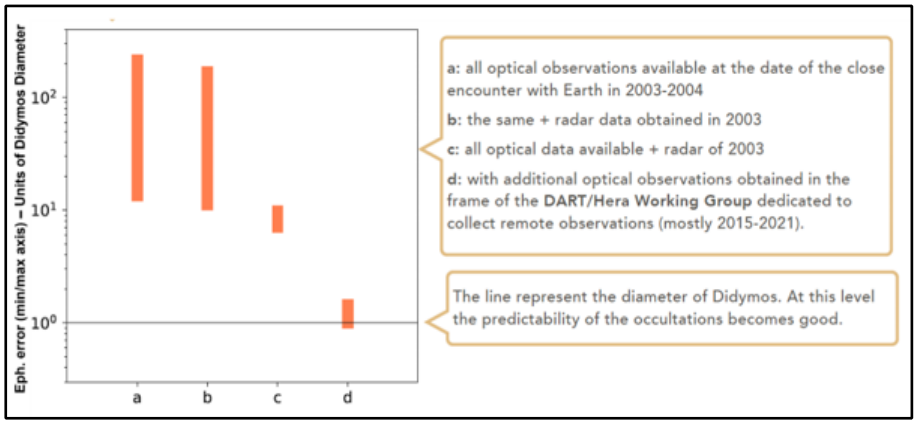

Figure 1. Figure showing the evolution of our knowledge on the eph. error. In scenario (d), we have finally reached "acceptable uncertainties" for the prediction of occultations.

Goals

Besides the occultation-derived astrometry mentioned above, we aim at measuring the sizes and shapes of these objects. Furthermore, in the case of Didymos, we keep (for now) an open mind on the possibility of measuring (using stellar occultations) the optical depth of the plume due to the *DART* impact.

The Predictions

In the framework of the ACROSS collaboration we have access to several telescopes, that will be used for the astrometric follow-up of the targets.

In our campaigns we will distinguish between:

• Objects for which we have high accuracy astrometry: For these objects, we will obviously be using our own improved orbital solution. That will be the case of Didymos, for example. Given that three members of the ACROSS team are also involved in the *DART*/*Hera* mission, we are using data obtained by the *DART* Investigation Team to make our own high accuracy astrometry and therefore a refined orbital solution.

• For most of the targets, especially in the third category mentioned above, we will be using the published orbital solution.

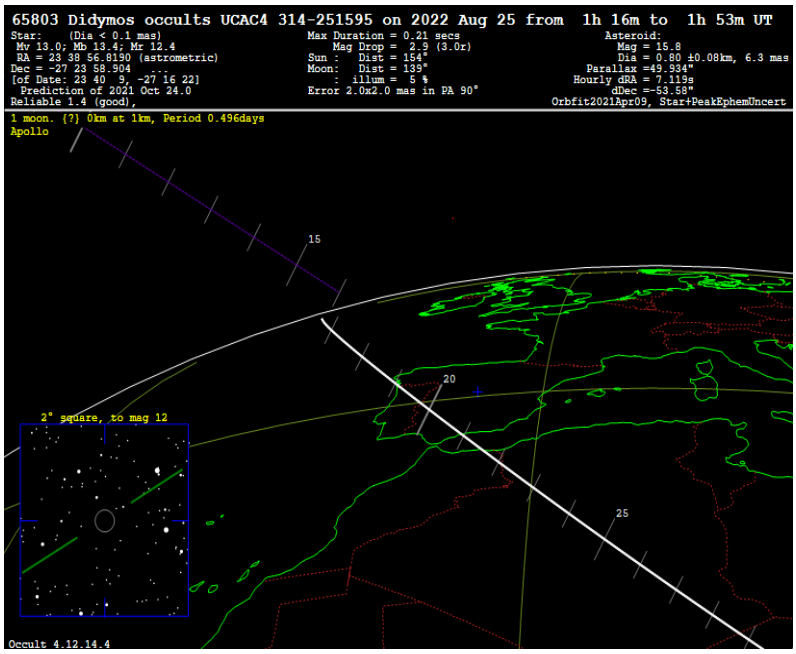

Figure 2. Didymos event observable in North Africa and Iberia on 2022/08/25, less than one month before the DART impact. (Occult v4.12.14.4)

Amongst our current collaborators we would like to mention the Lucky Star teams in Paris and Granada, as well Franck Marchis and the Unistellar Network.

The ACROSS team is reaching out to the International Occultation community through this announcement for a long, productive, and successful collaboration.

Clear Night Skies to all!

João Ferreira
ACROSS Team

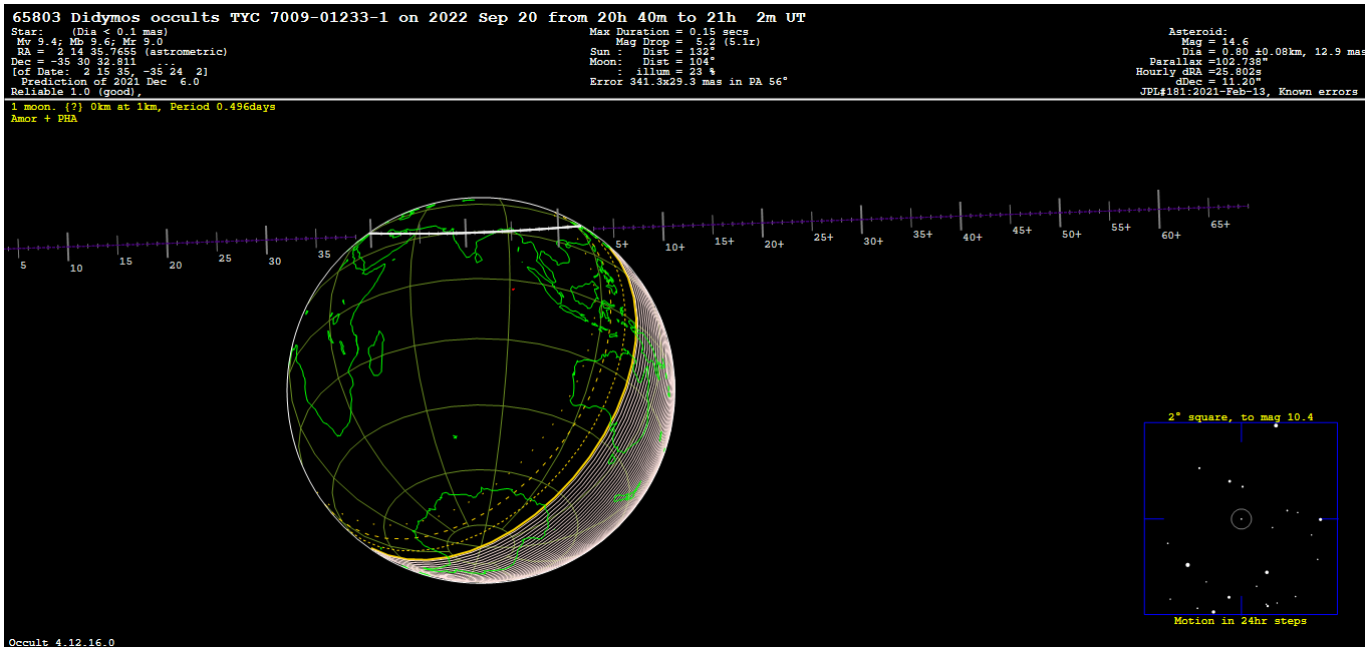

Figure 3. Didymos event observable in Asia on 2022/09/20, less than one week before the DART impact! (Occult v4.12.16.0)

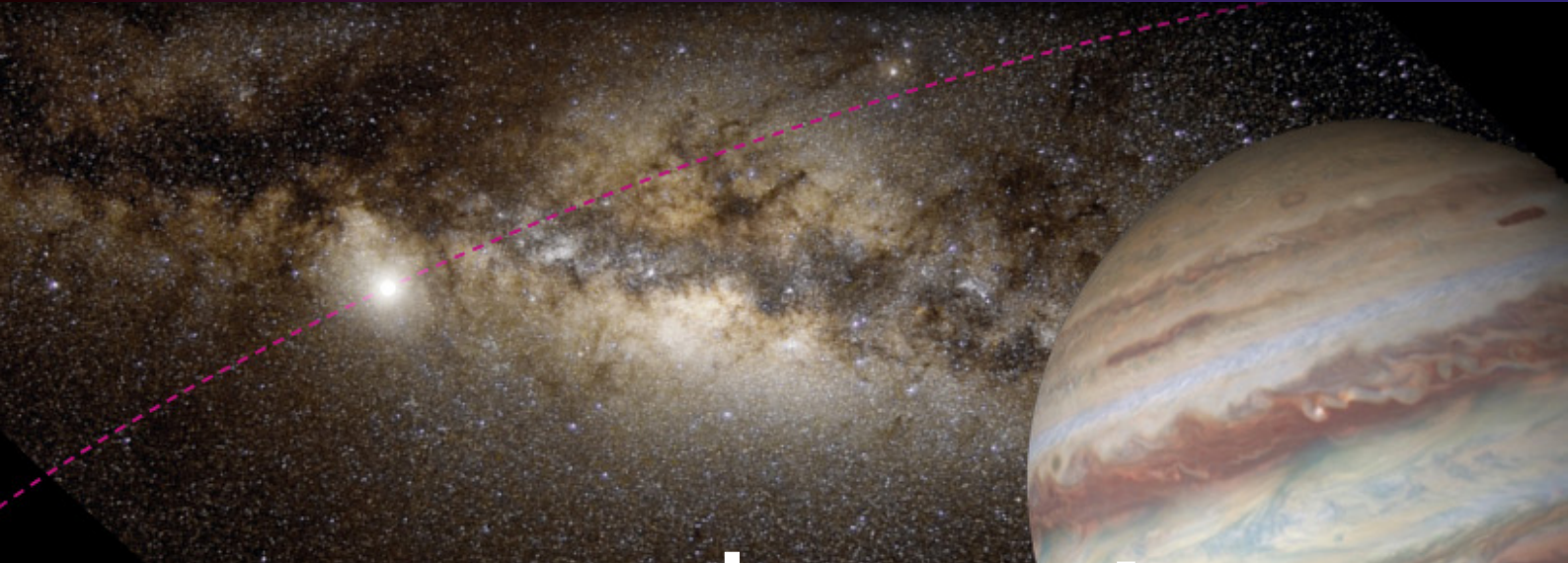

Beyond Jupiter

The World of Distant Minor Planets

Since the downgrading of Pluto in 2006 by the IAU, the planet Neptune marks the end of the zone of planets. Beyond Neptune, the world of icy large and small bodies, with and without an atmosphere (called Trans-Neptunian Objects or TNOs) starts. This zone between Jupiter and Neptune is also host to mysterious objects, namely the Centaurs and the Neptune Trojans. All of these groups are summarised as "distant minor planets". Occultation observers investigate these members of our solar system, without ever using a spacecraft. The sheer number of these minor planets is huge. As of 2022 March 27, the *Minor Planet Center* listed 1426 Centaurs and 2902 TNOs.

In the coming years, JOA wants to portray a member of this world in every issue; needless to say not all of them will get an article here. The table shows you where to find the objects presented in former JOA issues. (KG)

In this Issue:

(174567) Varda

Christian Weber · IOTA/ES · Berlin · Germany · camera@iota-es.de

ABSTRACT: (174567) Varda (former designation 2003 MW_{12}) is a binary Trans-Neptunian Object (TNO) located in the Kuiper Belt (Kuiper Belt Object, KBO). Varda was discovered in 2006 on images dated from 2003 obtained with the *Spacewatch* 0.9-m telescope at Kitt Peak. The secondary Ilmarë was discovered in 2009 using *Hubble Space Telescope* images. From the only known successful stellar occultation in 2018, Varda's apparent diameter was derived at 766 ± 6 km. Ilmarë is about half the size of Varda. Ilmarë's orbit around its main object (period 5.75 days) has a semi-major axis of about 4809 km. By 2027, 11 upcoming Varda stellar occultations are identified.

No.	Name	Author	Link to Issue
944	Hidalgo	Oliver Klös	JOA 1 2019
2060	Chiron	Mike Kretlow	JOA 2 2020
5145	Pholus	Konrad Guhl	JOA 2 2016
8405	Asbolus	Oliver Klös	JOA 3 2016
10370	Hylonome	Konrad Guhl	JOA 3 2021
10199	Chariklo	Mike Kretlow	JOA 1 2017
15760	Albion	Nikolai Wünsche	JOA 4 2019
15810	Awran	Konrad Guhl	JOA 4 2021
20000	Varuna	Andre Knöfel	JOA 2 2017
28728	Ixion	Nikolai Wünsche	JOA 2 2018
38628	Huya	Christian Weber	JOA 2-2021
47171	Lempo	Oliver Klös	JOA 4 2020

No.	Name	Author	Link to Issue
50000	Quaoar	Mike Kretlow	JOA 1 2020
54598	Bienor	Konrad Guhl	JOA 3 2018
55576	Amycus	Konrad Guhl	JOA 1 2021
60558	Echeclus	Oliver Klös	JOA 4 2017
90377	Sedna	Mike Kretlow	JOA 3 2020
90482	Orcus	Konrad Guhl	JOA 3 2017
120347	Salacia	Andrea Guhl	JOA 4 2016
134340	Pluto	Andre Knöfel	JOA 2 2019
136108	Haumea	Mike Kretlow	JOA 3-2019
136199	Eris	Andre Knöfel	JOA 1 2018
136472	Makemake	Christoph Bittner	JOA 4 2018
-	2004 XR_{190}	Carles Schnabel	JOA 1 2022

Figure 1. Kitt Peak National Observatory. The Steward Observatory with the Spacewatch 0.9-m telescope is the first from the left. Credit: Wikimedia Commons. Author: Joe Parks. Framing of https://commons.wikimedia.org/wiki/File:Kitt_Peak_National_Observatory_(1)_-_Flickr_-_Joe_Parks.jpg

The Discovery

(174567) Varda (former designation 2003 MW_{12}) was discovered by J. A. Larsen et al. in March 2006 on images dated from 2003 June 21 obtained with the Steward Observatory's *Spacewatch* 0.9-m telescope at Kitt Peak (Figure 1) [1]. According to MPC, precovery images date back to 1980. Currently, the last observation dates to 2021 June 6 [2].

In 2009, K. S. Noll et al. discovered Varda's secondary Ilmarë (former designation S/2009 (174567) 1) using *Hubble Space Telescope* (HST) images. This discovery was reported in 2011 [3]. Figure 2 shows a HST image of the Varda binary system.

Figure 2. Hubble Space Telescope image of Varda and Ilmarë. Credit: Wikimedia Commons Author: Hubble Space Telescope/Will Grundy; Processing: D. Bamberger. https://commons.wikimedia.org/wiki/File:Varda.gif

The Name

On 2014 January 16, the MPC published the name of 2003 MW_{12} as *Varda* and that of its satellite as *Ilmarë*: "In J. R. R. Tolkien's mythology, Varda is the queen of the stars, the star-kindler. She is the deity who, prior to the birth of the first humans, created the stars and constellations. She also set the vessels of the Sun and Moon upon their appointed courses above the girdle of the Earth. Ilmarë is Varda's handmaid." [4]. Figure 3 shows an artist's rendition of Varda.

Figure 3. Artist's rendition of Varda Elentári. Credit: Wikimedia Commons. Artist: Dominik Matus, own work. https://commons.wikimedia.org/wiki/File:Varda_Elent%C3%A1ri.jpg

Orbit and Classification

Varda's orbit around the Sun (Figure 4) has an inclination of 21.519 deg, a semi-major axis of 45.939 AU and an eccentricity of 0.145 (Epoch: JD 2459600.5, 2022 January 21) [5]. Varda's perihelion will be in 2094. Orbital classifications of TNOs are in some way ambiguous. So, according to DES classification (Deep Ecliptic

Survey) [6], M. W. Buie classifies Varda as "scattered–extended" [7] while the Minor Planet Center lists Varda only as "distant object" [2].

According to W. M. Grundy et al. [8] for Ilmarë, two possible orbit solutions exist (mirror-ambiguous orbit). The inclination of Ilmarë's orbit referenced to a J2000 equatorial frame is 101.0 ± 1.9 deg or 85.1 ± 1.8 deg. From the combination of the two solutions Grundy derives the semi-major axis to be 4809 ± 39 km, an eccentricity of 0.0215 and a period of 5.75 days (sidereal).

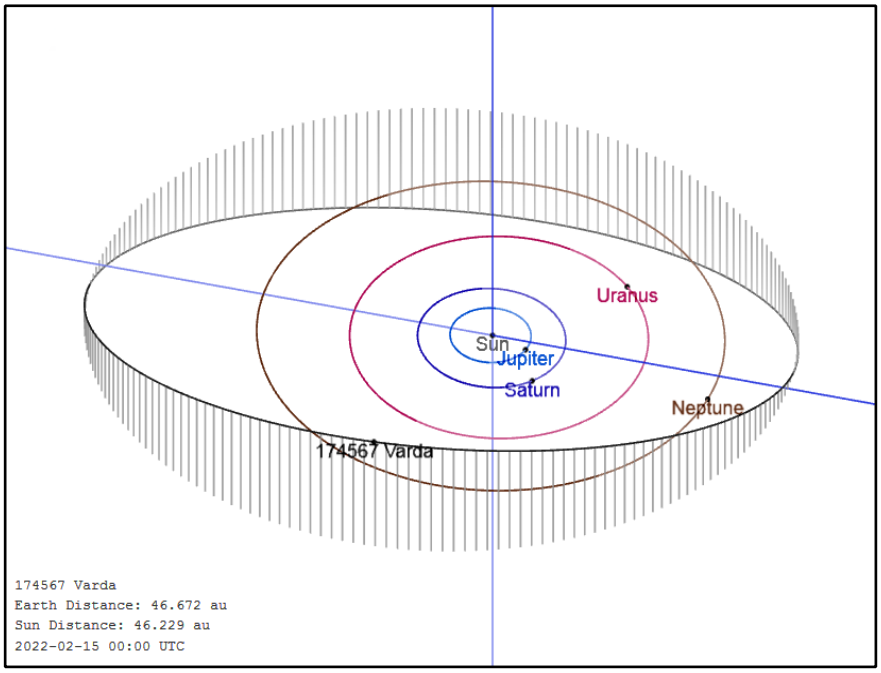

Figure 4. Varda's orbit diagram. Credit: JPL Small-Body Database Lookup [5]

Physical Characteristics

From the only successfully recorded stellar occultation to date (on 2018 September 10, see section Stellar Occultations), Varda was found to have an apparent diameter of 766 ± 6 km and an apparent oblateness of 0.066 ± 0.047. According to Souami et al. [9] the corresponding area-equivalent diameter is derived at 740 ± 14 km. Earlier measurements using different methods have similar results but larger uncertainties, see for example Grundy et al. 2015: 722 (+82 −76) km [8]. The stellar occultation also yields a geometric albedo of 0.099 ± 0.002 and a lack of evidence of an atmosphere [9].

So far Varda's rotation period could not be determined unambiguously. There are several solutions that lead to different results for the derived values. For the most probable rotation period of 5.91 h the bulk density yields to 1.78 ± 0.06 g/cm^3 and a true oblateness of 0.235 ± 0.05 [9].

According to the classification of Barucci et al. [10], visible colour photometry leads to the classification of Varda and its satellite in the group of IR objects. There is no evidence of water but of methanol ice [8].

After Charon, Dysnomia, Vanth and Hi'iaka, Ilmarë is the fifth-largest known moon of a TNO. According to conclusions by Souami et al. [9], Ilmarë's mean diameter is 356 km, whereas in 2015 Grundy et al. reported 326 (+38 −34) km [8]. So, Ilmarë is about half the size of its main body.

Space Mission Designs

NASA's *New Horizons* mission [11] has shown the great value of space missions to explore objects of the Kuiper Belt, e.g. (486958) Arrokoth, formerly called Ultima Thule/2014 MU$_{69}$. Several design studies for spacecraft missions targeting TNOs were proposed. For energy gain, most of the concepts use Jupiter flybys, some also gravity assists from Saturn and/or Uranus and Neptune. There are also unconventional propulsion concepts such as the use of fusion engines, which would make it possible to reach e.g. (136108) Haumea in only 6 years [12].

For example, Zangari et al. [13] identified launch opportunities for possible Varda missions with Jupiter swingbys from 2027 to 2031 and for 2039 to 2040. Depending on the energy per mass relation, the minimum flight duration ranges from 10.1 to 13.6 years.

A. Warren et al. [14] propose a Varda mission to launch on 2051 January 8 having a flight duration of 17 years and a final spacecraft mass of 2889 kg.

However, nothing is known about concrete plans to carry out a space mission to the Varda system.

Stellar Occultations

Time-resolved recordings of stellar occultations offer the possibility of determining the size and shape of occulting objects. Stellar occultations also allow the investigation of the object's surroundings to identify possible atmospheres, rings and satellites. A remarkable number of TNO results have been derived from stellar occultations. D. Herald's *Occult v4.2022.2.2* software [15] currently reports 53 TNO events (from 24 different objects) with at least one positive chord. The data is also available via NASA's Planetary Data System (PDS) [16]. The Lucky Star project [17] lists on its database (2005 to 2022 January 3) 96 TNO occultations (40 different objects) with at least one positive chord [18].

Varda's Stellar Occultation on 2018 Sep 10

Searching for Varda stellar occultation results one finds a negative (a single chord miss, recorded by C. Perello/A. Selva on 2015 September 13 [19]) and for the occultation of the star UCAC4 440-067774 (Mv 14.70) on 2018 September 15 a negative

result from Chile (E. Frappa/A. Klotz [20]) and 11 chords from the USA, including 5 positive ones. The campaign and the prediction were carried out within the Lucky Star project, the results are published in [9]. So far, Varda's satellite has not been detected by a stellar occultation. Figure 5 shows the 11 chords obtained in the USA.

Future Stellar Occultations

There are several resources for predicting stellar occultations by TNOs. S. Preston's/IOTA's high probability predictions list no Varda event until December 2022 [21].

Presently to 2023 January 1, the Lucky Star project offers predictions [22], usually having a high precision (NIMA ephemerides [23]). In the Gmag range up to 20 there are only two (low probability) Varda events [24], [25], see also Table 1. To optimize campaign planning, Lucky Star predictions appear in the "LuckyStar" feed of H. Pavlov's software *Occult Watcher* [26] and also in the *Occult Watcher Cloud* (OWC) [27].

Besides there is still M. W. Buie's "Global TNO event candidate list", containing TNO predictions up to eight years [28]. There are currently 13 events in Buie's list for Varda through 2028 November. Of them only 8 are crossing the Earth, they are listed in Table 1.

Table 1 also contains the author's predictions up to 2027 March using D. Herald's *Occult* software [15]. These predictions were made with JPL Horizons ephemerides of 2022 February 11 (solution #11 2021 July 9) and Gaia EDR3 data [29] for stars up to Mv 16. The author's predictions include Varda's satellite. All predictions suffer from large error ellipses.

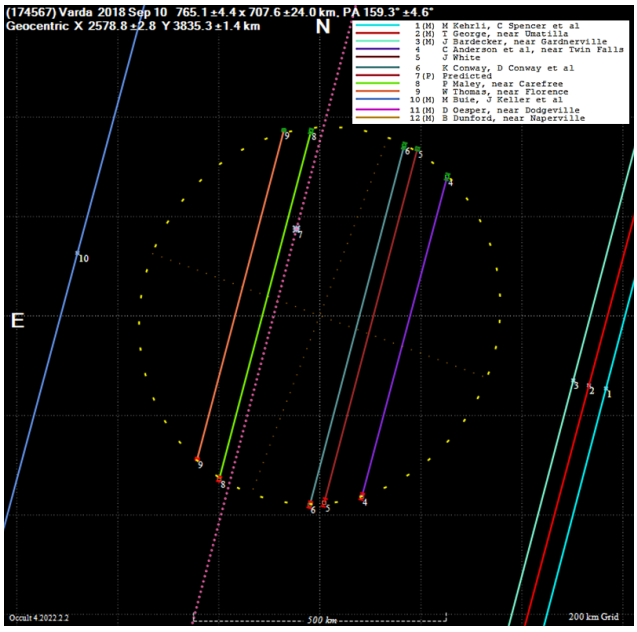

Figure 5. Varda's stellar occultation on 2018 September 10: Chords obtained in the USA. Credit: Occult v4.2022.2.2 [15]

Date	UT	Star Designation Gaia EDR3	Star Gmag	Max. Drn. [s]	Region	Source	Fig.
2022 Apr 30	21:54	4369535143805990528	18.5	0	Antarctica, S. Africa	LckSt	
2022 May 12	23:38	4369563151291377536	17.9	0	Arctic	LckSt	
2023 Mar 11	09:43	4370751517204786944	16.4	37.3	S. America	B	
2023 Mar 18	09:37	4370763817992674176 UCAC4 440-072597	15.0	58.2	*Varda:* M. America, Antarctica	Occ, B	Fig. 6
				30.1	*Ilmarë:* Newfoundland, S. America	Occ	Fig. 7
2023 Jun 1	06:02	4371028594132614656	16.0	21.4	S. S. America	B	
2023 Jun 26	13:03	4369544631391968256	16.3	20.9	E. Asia	B	
2024 Jun 10	17:50	4370812780619225088 UCAC4 443-075612	14.9	28.2	*Varda:* E. Asia, N. Africa	Occ, B	Fig. 8
				14.6	*Ilmarë:* Indonesia, Africa	Occ	Fig. 9
2025 Dec 24	05:48	4178436247629741312 UCAC4 438-075292	14.5	20.3	*Varda:* Arctic	Occ	Fig. 10
				10.4	*Ilmarë:* No Earth crossing	Occ	Fig. 11
2026 Jun 17	05:57	4178905532937521280	16.8	20.7	S. America	B	
2027 Jul 2	14:35	4178938930601092480	17.0	20.9	S. Asia	B	
2027 Jul 17	18:01	4178847563759686400	16.6	22.5	Greenland, Canada	B	

Table 1. Upcoming stellar occultations by (174567) Varda through 2027. "LckSt" Lucky Star predictions [22], "Occ" author's predictions with Occult v4.2022.2.2 [15] using JPL Horizons ephemerides (solution #11 2021 July 9) and Gaia EDR3 star data [29], "B" indicates M. W. Buie's predictions [28].

2023 Mar 18

Figure 6.

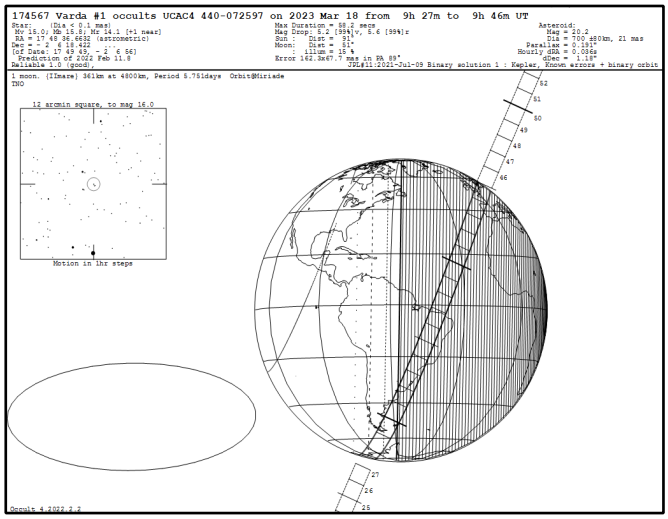

Figure 7.

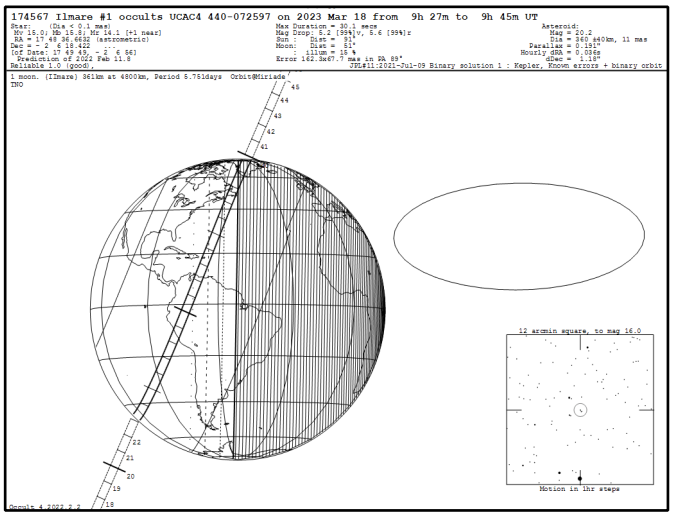

2024 Jun 10

Figure 8.

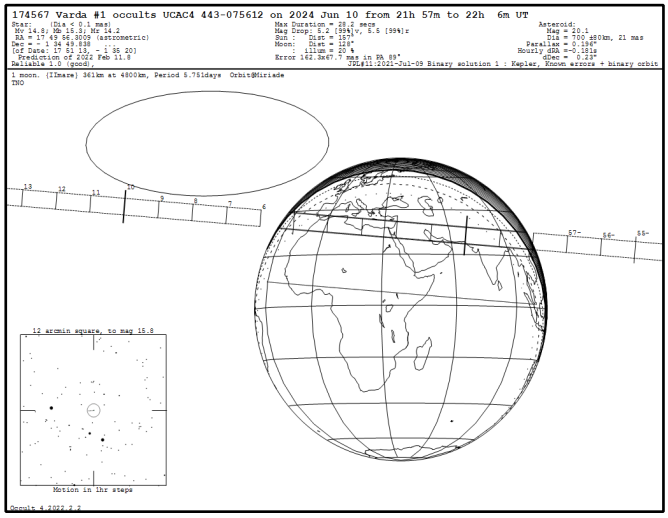

Figure 9.

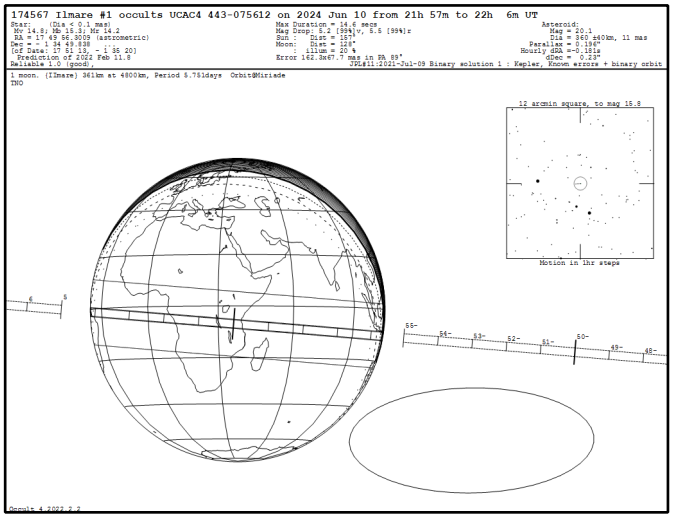

2025 Dec 24

Figure 10.

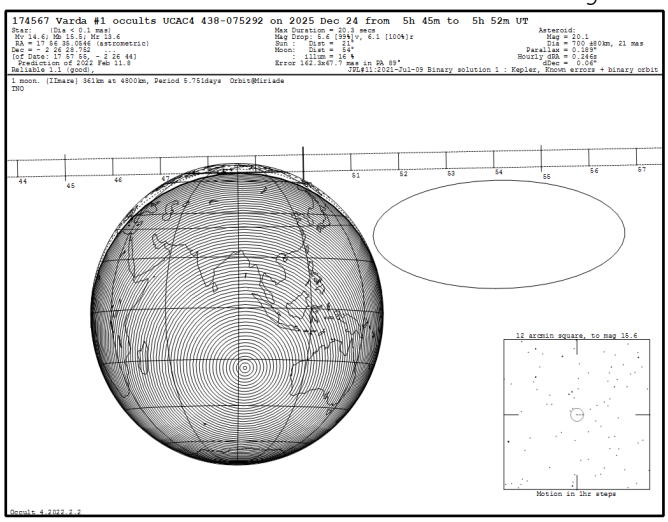

Figure 11.

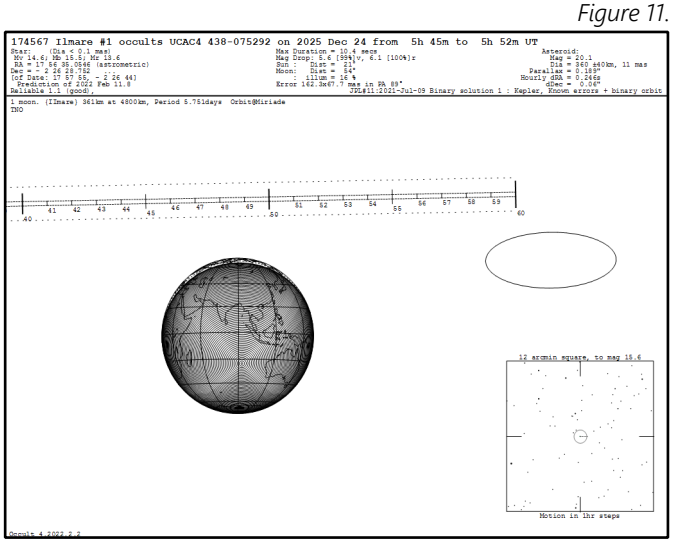

Figures 6 -11. Occultation maps according to Table 1. Credit: Occult v4.2022.2.2 [15]

Acknowledgements

This research has made use of data and/or services provided by the International Astronomical Union's Minor Planet Center. This work has made use of data from the European Space Agency (ESA) mission Gaia (https://www.cosmos.esa.int/gaia), processed by the Gaia Data Processing and Analysis Consortium (DPAC, https://www.cosmos.esa.int/web/gaia/dpac/consortium). Funding for the DPAC has been provided by national institutions, in particular the institutions participating in the Gaia Multilateral Agreement.

This research has made use of the VizieR catalogue access tool, CDS, Strasbourg, France (https://doi.org/10.26093/cds/vizier). The original description of the VizieR service was published in 2000, A&AS 143, 23. This research has made use of IMCCE's Miriade VO tool (https://ssp.imcce.fr/webservices/miriade/).

References

[1] Larsen, J. A. et al., The Search for Distant Objects in the Solar System Using Spacewatch. (2007) The Astronomical Journal. 133 (4): 1247–1270. https://doi.org/10.1086%2F511155

[2] MPC Database Search: Varda. https://www.minorplanetcenter.net/db_search/show_object?object_id=174567

[3] Noll, K. S. et al., (2011). Detection of eighteen trans neptunian binaries. Bull. Amer. Astron. Soc. 41, 1092 (abstract).

[4] M.P.C. 86715. Minor Planet Center. 2014 Jan 16. https://minorplanetcenter.net//iau/ECS/MPCArchive/2014/MPC_20140116.pdf

[5] JPL Small-Body Database Lookup: 174567 Varda (2003 MW12). Jet Propulsion Laboratory. https://ssd.jpl.nasa.gov/sbdb.cgi?sstr=174567

[6] Elliot, J. L. et al., (2005). The Deep Ecliptic Survey: A Search for Kuiper Belt Objects and Centaurs. II. Dynamical Classification, the Kuiper Belt Plane, and the Core Population. The Astronomical Journal. 129 (2): 1117–1162. https://doi.org/10.1086%2F427395

[7] Buie, M. W., The Deep Ecliptic Survey Object Classifications. SwRI. 2022 February 16. https://www.boulder.swri.edu/~buie/kbo/desclass.html

[8] Grundy, W. M. et al., (2015). The mutual orbit, mass, and density of the large transneptunian binary system Varda and Ilmare. Icarus. 257: 130–138. https://doi.org/10.1016%2Fj.icarus.2015.04.036

[9] Souami, D. et al., (August 2020). A multi-chord stellar occultation by the large trans-Neptunian object (174567) Varda. Astronomy & Astrophysics. 643: A125. arXiv:2008.04818. https://doi.org/10.1051/0004-6361/202038526

[10] Barucci, M. A. et al., (September 2005). Taxonomy of Centaurs and Trans-Neptunian Objects. The Astronomical Journal, Volume 130, Issue 3, pp. 1291-1298. https://iopscience.iop.org/article/10.1086/431957

[11] NASA. New Horizons. https://www.nasa.gov/mission_pages/newhorizons/main/index.html

[12] Aime, P. et al., Exploration of trans-Neptunian objects using the Direct Fusion Drive. (2021) Acta Astronautica, 178 , pp. 257-264. https://doi.org/10.1016/j.actaastro.2020.09.022

[13] Zangari, A. M. et. al., Return to the Kuiper Belt: launch opportunities from 2025 to 2040. Journal of Spacecraft and Rockets, vol. 56, issue 3, pp. 919-930. (May 2019). https://doi.org/10.2514/1.A34329

[14] Warren, A. et al., (2021). AAS 21-763 Multiple Observation Opportunities for Trans-Neptunian Objects Part 8. https://www.researchgate.net/publication/355583728

[15] Herald, D., Occult v4.11.x.x. Occultation Prediction Software. (Current version 4.2022.2.15). http://www.lunar-occultations.com/iota/occult4.htm

[16] Herald, D. et al., Asteroid Occultations V3.0. urn:nasa:pds:smallbodiesoccultations::3.0. NASA Planetary Data System, (2019). https://sbn.psi.edu/pds/resource/occ.html

[17] ERC Lucky Star project. https://lesia.obspm.fr/lucky-star/

[18] Braga-Ribas, F. et al., (2019). Database on detected stellar occultations by small outer Solar System objects. J. Phys.: Conf. Ser. 1365 012024. https://iopscience.iop.org/article/10.1088/1742-6596/1365/1/012024 Database: http://occultations.ct.utfpr.edu.br/results/#tno

[19] Frappa, E., euraster.net. European Asteroidal Occultation Results. http://www.euraster.net/results/2015/index.html#0913-174567

[20] Frappa, E. euraster.net. European Asteroidal Occultation Results. http://www.euraster.net/results/2018/index.html#0910-174567

[21] Preston, S., Monthly Index of Asteroid Occultation Path Predictions. http://www.asteroidoccultation.com/IndexAll.htm

[22] Predictions of stellar occultations by TNOs and Centaurs. ERC Lucky Star project. https://lesia.obspm.fr/lucky-star/predobs.php?lon=13&lat=52

[23] Desmars, J. et al., (September 2015). Orbit determination of Transneptunian objects and Centaurs for the prediction of stellar occultations. A&A 584, A96 (2015). https://arxiv.org/abs/1509.08674

[24] Occultation by Varda (2022-04-30). ERC Lucky Star project. https://lesia.obspm.fr/lucky-star/occobs.php?p=80831&lon=13&lat=52

[25] Occultation by Varda (2022-05-12). ERC Lucky Star project. https://lesia.obspm.fr/lucky-star/occobs.php?p=80832&lon=13&lat=52

[26] Pavlov, H., OccultWatcher 5.0. (Current version 5.0.0.5). http://www.occultwatcher.net/

[27] Pavlov, H., Occult Watcher Cloud (OWC). https://cloud.occultwatcher.net/

[28] Buie, M. W., Global TNO event candidate list. SwRI. 2022 February 13. https://www.boulder.swri.edu/~buie/recon/allevents.html

[29] Gaia Early Data Release 3. European Space Agency. https://www.cosmos.esa.int/web/gaia/early-data-release-3

Invitation to ESOP 2022 in Granada (Andalucía/Spain)

The 41th European Symposium on Occultation Projects (ESOP) will take place in Granada, Spain, from Saturday 10 to Sunday 11 September 2022. Following the symposium we will offer a social programme including a visit to the *Calar Alto Observatory*, www.caha.es, near Almería.

ESOP will take place one week before the Europlanet Science Congress (EPSC), to be held in Granada as well on 18-23 September, where up to 1,000 both professional and amateur astronomers from around the world are expected to participate, thus offering you the possibility to attend both conferences with a week of recreation in-between in the beautiful region of Andalucía. Moreover, this will be a good opportunity to enhance the pro-am link in the domain of occultation astronomy.

Granada is the capital of the Granada province in Andalucía, Spain, and is located at the foot of the Sierra Nevada mountains. However, it is also only one hour by car from the Mediterranean coast and about 1.5 hours from the city of Málaga. Granada is also well known within Spain for the University of Granada which has about 80,000 students, forming a significant part of the total population of the city. Granada has a lot to offer in terms of infrastructure (accommodation, travelling), culture, food (tapas!), sightseeing, nature and science.

Details and Registration here:
https://esop41.iota-es.de

Credit: IAA-CSIC

Currently, we are expecting that the symposium will take place in person, but we are also planning to offer some virtual support like streaming of the lectures. Details about this hybrid mode will be available on the web page.

The exact venue of the conference is still under investigation and will depend on the pandemic situation as well as the number of registered attendees, and will be announced as soon as possible on the webpage and by e-mail.

We are looking forward to welcome you in the wonderful city of Granada!

Mike Kretlow
Pablo Santos-Sanz
IAA (LOC/SOC)

IAA INSTITUTO DE ASTROFÍSICA DE ANDALUCÍA CSIC

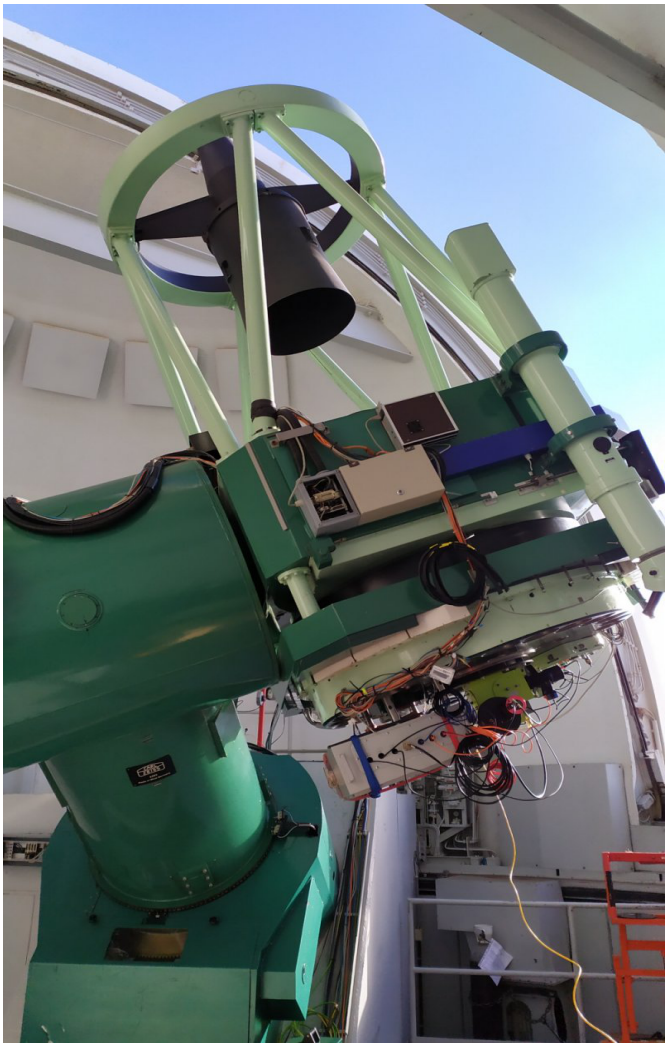

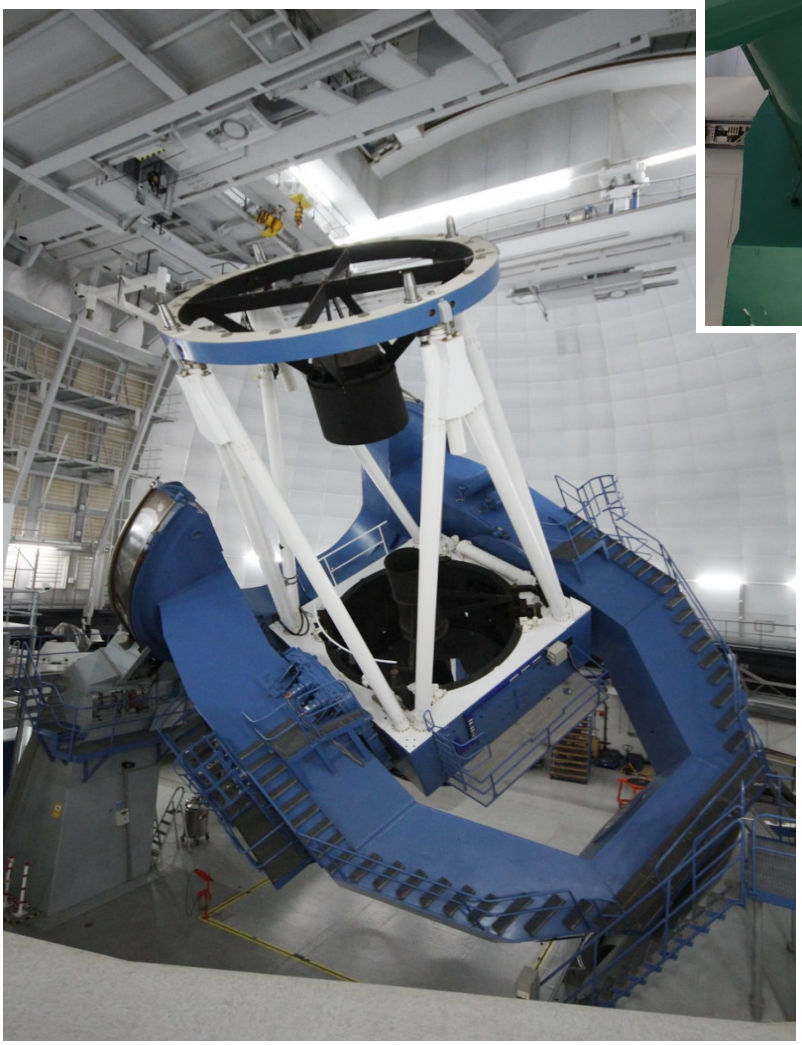

The German-Spanish Astronomical Center at Calar Alto is located in the Sierra de Los Filabres (Andalucía, Southern Spain) north of Almería. It is operated jointly by the Junta de Andalucía and the Instituto de Astrofísica de Andalucía (CSIC) in Granada/Spain.
Calar Alto provides three telescopes with apertures of 1.23 m (top), 2.2 m and 3.5m (left) to the general community. A 1.5 m-telescope, also located on the mountain, is operated under the control of the Observatory of Madrid.
Credit of images Calar Alto: M. Kretlow
Credit caption: https://www.caha.es/about-caha mainmenu-93 introduction-mainmenu-49

Journal for
Occultation
Astronomy

IOTA's Mission

The International Occultation Timing Association, Inc was established to encourage and facilitate the observation of occultations and eclipses It provides predictions for grazing occultations of stars by the Moon and predictions for occultations of stars by asteroids and planets, information on observing equipment and techniques, and reports to the members of observations made.

The Journal for Occultation Astronomy (JOA) is published on behalf of IOTA, IOTA/ES and RASNZ and for the worldwide occultation astronomy community.

Worldwide Partners

Club Eclipse (France). . . . . www.astrosurf.com/club_eclipse
IOTA-India . . . . . http://iota-india.in
IOTA/ME (Middle East) . . . . . www.iota-me.com
President: Atila Poro . . . . . iotamiddleeast@yahoo.com
LIADA (Latin America) . . . . . www.ocultacionesliada.wordpress.com
SOTAS (Stellar Occultation Timing Association Switzerland) . . . . . www.occultations.ch

Imprint

Publisher: IOTA/ES, Am Brombeerhag 13, D-30459 Hannover, Germany
Responsible in Terms of the German Press Law (V.i.S.d.P.): Konrad Guhl

Editorial Board: Wolfgang Beisker, Oliver Klös, Alexander Pratt, Carles Schnabel, Christian Weber
Additional Reviewers: David W. Dunham, Richard Miles Contact: joa@iota-es.de
Layout Artist: Oliver Klös Original Layout by Michael Busse (†)

Webmaster: Wolfgang Beisker, wbeisker@iota-es.de

JOA Is Funded by Membership Fees (Year): IOTA: US$15.00 IOTA/ES: €20.00 RASNZ: NZ$35.00

Publication Dates: 4 times a year

Submission Deadline for JOA 2022-3: May 15

IOTA maintains the following web sites for your information and rapid notification of events:

www.occultations.org
www.iota-es.de
www.occultations.org.nz

These sites contain information about the organisation known as IOTA and provide information about joining.

The main page of occultations.org provides links to IOTA's major technical sites, as well as to the major IOTA sections, including those in Europe, Middle East, Australia/New Zealand, and South America.

The technical sites hold definitions and information about all issues of occultation methods. It contains also results for all different phenomena. Occultations by the Moon, by planets, asteroids and TNOs are presented. Solar eclipses as a special kind of occultation can be found there as well results of other timely phenomena such as mutual events of satellites and lunar meteor impact flashes.

IOTA and IOTA/ES have an on-line archive of all issues of Occultation Newsletter, IOTA'S predecessor to JOA.

Journal for Occultation Astronomy

(ISSN 0737-6766) is published quarterly in the USA by the International Occultation Timing Association, Inc. (IOTA)
PO Box 20313, Fountain Hills, AZ 85269-0313

IOTA is a tax-exempt organization under sections 501(c)(3) and 509(a)(2) of the Internal Revenue Code USA, and is incorporated in the state of Texas. Copies are distributed electronically.

Regulations

The Journal of Occultation Astronomy (JOA) is not covenanted to print articles it did not ask for.

The author is responsible for the contents of his article & pictures.

If necessary for any reason JOA can shorten an article but without changing its meaning or scientific contents.

JOA will always try to produce an article as soon as possible based to date & time of other articles it received – but actual announcements have the priority!